CHEMISTRY
A EUROPEAN JOURNAL

DOI: 10.1002/chem.201001253

Synthesis and Molecular Modelling of Double-Functionalised Nucleosides with Aromatic Moieties in the 5′-(*S*)-Position and Minor Groove Interactions in DNA Zipper Structures

Khalil Isak Shaikh, Charlotte Stahl Madsen, Lise Junker Nielsen, Anna Søndergaard Jørgensen, Henrik Nielsen, Michael Petersen, and Poul Nielsen*[a]

Abstract: A series of six double-functionalised nucleosides, in which aromatic moieties were inserted into the 5′-(*S*)-*C*-position, were synthesised and incorporated into DNA duplexes. The aromatic moieties were thymine-1-yl, phenyl, 1,2,3-triazol-1-yl, 1,2,3-triazol-4-yl, 4-(uracil-5-yl)-1,2,3-triazol-1-yl and 4-phenyl-1,2,3-triazol-1-yl. The DNA duplexes were studied with UV melting curves, CD spectroscopy and molecular modelling. The results showed that the aromatic moieties in some cases interact in the minor groove forming DNA zipper structures. The strongest specific interaction was found between two thymines or between a thymine and a phenyl group in a crossed (−3)-zipper motif (i.e., with two base pairs interspacing the modifications). Modelling revealed that the interaction is aromatic stacking across the minor groove. Also, the extended uracil-triazole moiety demonstrated zipper contacts in the minor groove as well as binding to the floor of the groove.

Keywords: click chemistry · DNA · molecular recognition · nanobiotechnology · stacking interactions

Introduction

The DNA double helix constitutes an excellent scaffold for supramolecular design.[1] Various entities have been organised on the surface of the duplex,[2] for instance, a range of different aromatic chromophores,[3] often with the nucleobases as the starting point for derivatisation.[2,3] Recently we and others have pursued the idea that nucleosides with additional nucleobases, so-called double-headed nucleosides, could be useful tools for: 1) organising additional nucleobases on the duplex surface to make intra- or extrahelical contacts by base pairing or stacking, and 2) for the design of oligonucleotides targeting various nucleic acid secondary structures.[4–10] For the latter purpose, we obtained promising stabilisation of a three-way junction with our first double-headed nucleoside presenting an additional thymine in the 2′-position, 2′-deoxy-2′-*C*-(2-(thymin-1-yl)ethyl)uridine (**1**, Scheme 1).[4] For the former purpose, we have demonstrated promising results with the double-headed nucleoside **2**, 5′-(*S*)-*C*-(thymin-1-yl)methylthymidine, which positions an additional thymine into the minor groove of a duplex.[5] When **2** was introduced in DNA duplexes, slight thermal destabilisation of these as compared to unmodified duplexes was observed. When two double-headed nucleosides **2** were incorporated in complementary DNA sequences with two interspacing base pairs (a so-called (−3)-zipper motif), a base–base stacking interaction between the two additional thymines was observed to lead to a relative stabilisation of the duplex.[5] This zipper interaction was consistent and specific

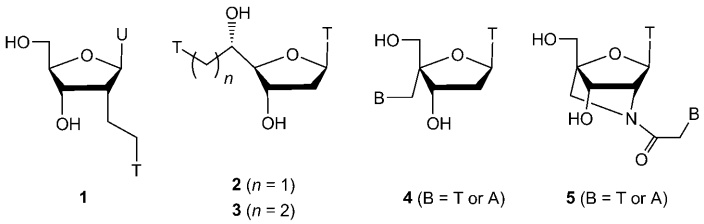

1 **2** (*n* = 1) **3** (*n* = 2) **4** (B = T or A) **5** (B = T or A)

Scheme 1. Double-headed nucleosides: T = thymin-1-yl; U = uracil-1-yl; A = adenin-9-yl.

[a] Dr. K. I. Shaikh, C. S. Madsen, L. J. Nielsen, A. S. Jørgensen, H. Nielsen, Prof. Dr. M. Petersen, Prof. Dr. P. Nielsen
Nucleic Acid Center, Department of Physics and Chemistry
University of Southern Denmark, Campusvej 55
5230 Odense M (Denmark)
Fax: (+45) 6615-8780
E-mail: pon@ifk.sdu.dk

Supporting information for this article is available on the WWW under http://dx.doi.org/10.1002/chem.201001253.

for (−3)-zippers. In a later study we investigated a longer ethylene linker between the thymine and the 5′-*C*-position (**3**, Scheme 1).[6] However, no zipper interactions were observed, probably due to the increased flexibility.

Double-headed nucleosides with the additional base in the 4′-position (**4**)[7] as well as 2′-amino-LNA with an additional base linked to the amino group (**5**)[8] have been introduced in both strands of a DNA duplex. Both adenine and thymine derivatives were prepared, but the interactions found in the minor groove were weak in both cases.[7,8] Acyclic double-headed nucleosides have also been studied as building blocks in DNA, but the flexibility of the acyclic backbone in all cases led to pronounced destabilisation of the duplexes.[9–10]

Here, we investigate the scope of the (−3)-zipper interaction found with **2** by the variation of sequence context and by alteration of the additional nucleobase in the 5′-position. Hereby, we can deduce if the stacking in the minor groove is restricted to thymine and whether other contacts in or across the minor groove can be found. Firstly, we decided to replace the thymine with a simple phenyl group, and secondly, we decided to use Cu-catalysed [3+2]cycloaddition between terminal alkynes and azides (CuAAC)[11] to give a small series of 1,2,3-triazoles. By variation of the substitution pattern of the triazole, interactions by triazole itself or by aromatic substituents can be studied. Hence, we decided to place a uracil as well as a phenyl at the triazole. The six double-headed nucleotides of the current study are shown in Scheme 2.

Results and Discussion

Chemical synthesis: The chemical synthesis of **2**[5] as well as of four of the five new 5′-*C*-modified nucleotides

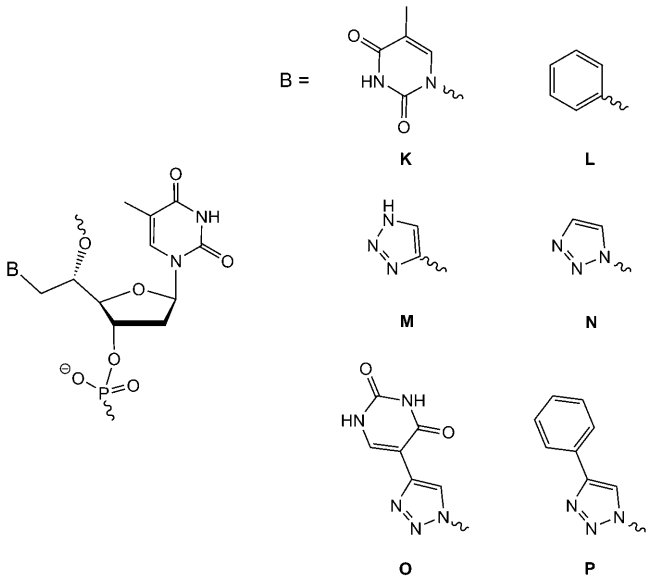

Scheme 2. Double-functionalised nucleotide monomers **K**–**P**; **K** corresponds to the incorporation of **2**.

(Scheme 2) was based on nucleophilic ring opening of the 5′-epoxide **6** (Scheme 3). This epoxide had been obtained in three steps from 3′-*O*-(*tert*-butyldimethylsilyl)thymidine.[5,12] Oxidation and Wittig olefination gave the 5′-methylene derivative in high yield, whereas the final mCPBA-mediated oxidation of the alkene gave **6** as the pure 5′ (*S*)-isomer in a more modest 42% yield.[5] Several attempts failed to improve on the epoxidation, including mCPBA oxidation under microwave irradiation, Payne oxidation,[13] methyltrioxorhenium(VII) (MTO), H_2O_2 and pyridine,[14] as well as DCC and H_2O_2.[15]

The original double-headed nucleoside **2** was prepared by nucleophilic opening of the epoxide **6** by thymine in a good yield.[5] The phenyl group was introduced by using a similar strategy with the Grignard reagent, phenylmagnesium bromide, in combination with copper(I) iodide,[16] and after pixylation the 5′-*C*-benzylthymidine derivative **7** was obtained in 47% over two steps. An attempt at synthesising **7** by using BnMgBr and 3′-*O*-(*tert*-butyldimethylsilyl)thymidine-5′-aldehyde failed. Deprotection of the 3′-hydroxyl group afforded **8** and subsequent phosphitylation gave the desired phosphoramidite **9** for the incorporation of monomer **L** into oligonucleotides.

The corresponding phosphoramidites for incorporating monomers **N**, **O** and **P** were synthesised by the CuAAC reaction.[11] Introduction of the azido group in **6** by using a known protocol gave **10**,[12] and protection of the 5′-hydroxy group by pixylation gave the key azide substrate, **11**. Formation of the triazole derivatives was achieved by using phenylacetylene, *N*1-benzoyl-5-ethynyluracil, which was made from 5-(trimethylsilyl)ethynyluracil[17] (see the Supporting Information), and trimethylsilylacetylen to give the nucleosides **12**, **15** and **18**, respectively, in high yields (81–97%). Subsequent deprotection of the 3′-hydroxy groups with TBAF afforded the nucleosides **13**, **16** and **19** in satisfactory yields, which after phosphitylation gave the phosphoramidites **14**, **17** and **20** in 25, 35 and 36% overall yield (from **11**), respectively.

Finally, the phosphoramidite for incorporating monomer **M** was synthesised from 3′-*O*-(*tert*-butyldimethylsilyl)-5′-(*S*)-*C*-propagylthymidine (**21**), which was obtained from 3′-*O*-(*tert*-butyldimethylsilyl)thymidine by using a recently published procedure.[18] The protected triazole **22** was obtained in very high yield (97%) through CuAAC by using an in situ azidation procedure.[19] Furthermore, pixylation of the 5′-hydroxy group moiety gave **23** in 92% yield, and deprotection of the 3′-hydroxy group and phophitylation gave phosphoramidite **25** in 36% overall yield (from **21**).

The phosphoramidites **9**, **14**, **17**, **20** and **25**, as well as the known phosphoramidite of **2**,[5] were incorporated in oligonucleotides (ONs) to give the monomers **L**, **P**, **O**, **N**, **M** and **K**, respectively, by using standard solid phase DNA synthesis with 1*H*-tetrazole as the activator. The coupling yields were >90% for all phosphoramidites, and the standard acetic treatment after each coupling procedure removed the pixyl group. The final deprotection and removal of the ONs from the solid support with concentrated aqueous ammonia

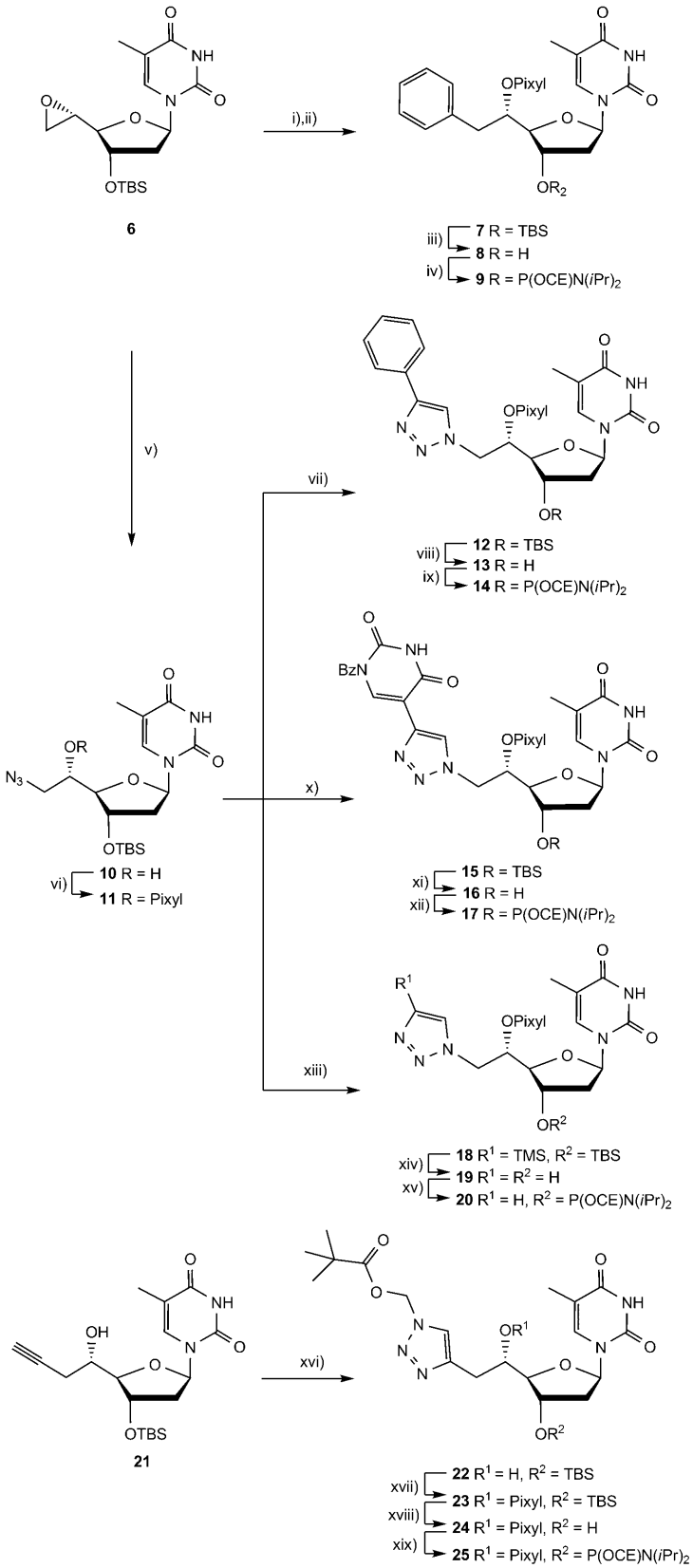

also removed the benzoyl group of **17** (to give monomer **O**) and the pivaloyloxymethyl group of **25** (to give monomer **M**). The constitution and purity of the ONs was verified by MALDI-MS (Table S1 in the Supporting Information) and ion exchange/RF-HPLC.

Hybridisation studies: The six 5′ modified nucleotide monomers, **K**–**P**, were each incorporated into six 11-mer ONs (X1–X6, Table 1). The sequence context was the same as that already studied with monomer **K**,[5,6] and complementary sequences were used with the monomers introduced once or twice in various positions to study potential zipper motifs. Entries 1–6 in Table 1 show the effects on duplex stability of one or two incorporation(s) in the same strand of either of the monomers, **K**–**P**. With the incorporation of monomer **K**[5] the data show a uniform decrease in duplex stability of −4.4 to −6.0 °C for each modified monomer as compared to the unmodified duplex. The most pronounced decrease was seen with two incorporations in the same strand (entry 6). With the incorporation of **L**, which has a phenyl ring instead of a thymine, similar, but in all cases, smaller decreases in duplex stability were obtained (ΔT_m values between −3.2 and −4.8 °C). In other words, the monomer **L** is slightly better accommodated in duplexes than **K**. The incorporation of monomers **M** and **N**, displaying triazoles in the minor groove, showed decreases in duplex stability, but whereas monomer **N** demonstrated decreases in duplex stability that are very similar to the results obtained with **K** (ΔT_m values between −4.4 and −5.8 °C), **M** displayed somewhat more stable duplexes (ΔT_m values between −1.0 and −3.6 °C). Hence, the more hydrophilic **M** with a distal NH is better accommodated in the duplexes than the more hydrophobic **N** with a distal CH moiety. Incorporation of the two larger monomers **O** and **P** displaying triazoles connected to either a uracil or a phenyl, respectively, in general displayed a more pronounced decrease in duplex stability, with ΔT_m values between −6.6 and −9.7 °C observed for **P**, and between −7.7 and −9.4 °C for **O**. However, a remarkable exception is entry 4 with a ΔT_m of only −1.6 °C. This might be due to a sequence specific contact in the bottom of the minor groove from the additional uracil moiety (see below). In general, the six different nucleotides gave rise to destabi-

Scheme 3. i) CuI, PhMgBr, THF, −78 °C; ii) PixylCl, pyridine, 47% over two steps; iii) TBAF, THF, 86%; iv) $NC(CH_2)OP(Cl)N(iPr)_2$, DIPEA, DCE, 47%; v) NaN_3, DMF, 55 °C, 80%; vi) PixylCl, DMAP, MW 120 °C, 72%; vii) phenylacetylene, sodium ascorbate, $CuSO_4$, *t*BuOH-H_2O-pyridine, 92%; viii) TBAF, THF, 70%; ix) $NC(CH_2)OP(Cl)N(iPr)_2$, DIPEA, DCM, 54%; x) 1*N*-benzoyl-5-ethynyluracil, sodium ascorbate, $CuSO_4$, *t*BuOH-H_2O-pyridine, 81%; xi) TBAF, THF, 86%; xii) $NC(CH_2)OP(Cl)N(iPr)_2$, DIPEA, DCM, 70%; xiii) TMS-acetylene, sodium ascorbate, $CuSO_4$, *t*BuOH-H_2O-pyridine, 88%; xiv) TBAF, THF, 94%; xv) $NC(CH_2)OP(Cl)N(iPr)_2$, DIPEA, DCM, 60%; xvi) NaN_3, pivaloylmethyl chloride, sodium ascorbate, CuI, *t*BuOH-H_2O, DMEDA, MW 120 °C, 97%; xvii) PixylCl, pyridine, 92%; xviii) TBAF, THF, 57%; xix) $NC(CH_2)OP(Cl)N(iPr)_2$, DIPEA, DCM, 70%. CE = cyanoethyl; TBS = *tert*-butyldimethylsilyl; pixyl = 9-phenylxanthen-9-yl; TMS = trimethylsilyl.

Table 1. Thermal stability data for modified DNA duplexes.

Entry	Possible zipper	ONs (**x**:**y**)	Duplex	**X** =	ΔT_m [°C][a] ($\Delta\Delta T_m$ [°C])[b] **K**[c]	**L**	**M**	**N**	**O**	**P**
1		T1 X1	5′-d(CGC ATA TTC GC) 3′-d(GCG **X**AT AAG CG)		−5.4	−3.2	−2.7	−4.4	−7.7	−6.9
2		T1 X2	5′-d(CGC ATA TTC GC) 3′-d(GCG TA**X** AAG CG)		−4.7	−3.8	−3.6	−5.3	−9.4	−7.3
3		T1 X3	5′-d(CGC ATA TTC GC) 3′-d(GCG **X**A**X** AAG CG)		−10.9	−7.2	−6.9	−9.2	−16.3	−17.4
4		X4 T2	5′-d(CGC ATA T**X**C GC) 3′-d(GCG TAT AAG CG)		−4.4	−3.5	−1.0	−5.3	−1.6	−6.6
5		X5 T2	5′-d(CGC ATA **X**TC GC) 3′-d(GCG TAT AAG CG)		−4.9	−4.5	−1.4	−5.8	−7.8	−7.5
6		X6 T2	5′-d(CGC A**X**A **X**TC GC) 3′-d(GCG TAT AAG CG)		−12.0	−9.5	−5.7	−11.0	−16.0	−19.3
7	(−1)	X5 X2	5′-d(CGC ATA **X**TC GC) 3′-d(GCG TA**X** AAG CG)		−10.4 (−0.8)	−8.1 (+0.1)	−5.1 (−0.1)	−10.0 (+1.1)	−15.2 (+2.0)	−12.9 (+1.9)
8	(−2)	X4 X2	5′-d(CGC ATA T**X**C GC) 3′-d(GCG TA**X** AAG CG)		−10.0 (−0.9)	−5.2 (+2.2)	−3.2 (+1.4)	−7.4 (+3.2)	−4.4 (+6.6)	−7.5 (+6.4)
9	(−3)	X5 X1	5′-d(CGC ATA **X**TC GC) 3′-d(GCG **X**AT AAG CG)		−3.8 (+6.5)	−6.3 (+1.4)	−4.2 (−0.1)	−8.7 (+1.5)	−10.7 (+4.8)	−13.8 (+0.6)
10	(−4)	X4 X1	5′-d(CGC ATA T**X**C GC) 3′-d(GCG **X**AT AAG CG)		−9.8 (0.0)	−8.3 (−1.6)	−3.8 (−0.1)	−7.5 (+2.2)	−8.4 (−0.1)	−11.3 (+2.2)
11	(−2)(−4)	X4 X3	5′-d(CGC ATA T**X**C GC) 3′-d(GCG **X**A**X**AAG CG)		−17.0 (−1.7)	−9.5 (+1.2)	−7.0 (+0.9)	−10.3 (+4.2)	−9.6 (+8.3)	−15.6 (+8.4)
12	(−1)(−3)	X5 X3	5′-d(CGC ATA **X**TC GC) 3′-d(GCG **X**A**X** AAG CG)		−9.0 (+6.8)	−10.2 (+1.5)	−6.9 (+1.4)	−12.8 (+2.2)	−20.2 (+3.9)	−16.0 (+8.9)
13	(−3)(−1)	X6 X1	5′-d(CGC A**X**A **X**TC GC) 3′-d(GCG **X**AT AAG CG)		−10.4 (+7.0)	−12.7 (+1.1)	−10.1 (−1.7)	−13.1 (+2.3)	−16.5 (+7.2)	−21.4 (+4.8)
14	(−1)(+1)	X6 X2	5′-d(CGC A**X**A **X**TC GC) 3′-d(GCG TA**X** AAG CG)		−18.2 (−1.5)	−16.3 (−3.0)	−11.6 (−2.3)	−14.9 (+1.4)	−16.3 (+9.1)	−26.3 (+3.0)
15	(−1)(−3)(+1)(−1)	X6 X3	5′-d(CGC A**X**A **X**TC GC) 3′-d(GCG **X**A**X** AAG CG)		−16.8 (+6.1)	−16.2 (+0.5)	−12.7 (−0.1)	−16.5 (+3.7)	−11.4 (+20.9)	−22.5 (+14.2)

[a] Differences in melting temperatures compared to the unmodified duplex (T1:T2); $\Delta T_{m(x:y)} = T_{m(x:y)} - T_{m(T1:T2)}$. Melting temperatures ($T_m$, °C) were obtained from the maxima of the first derivatives of the melting curves (A_{260} vs. temperature) recorded in a medium salt buffer (Na_2HPO_4/NaH_2PO_4, 7.5 mM with respect to phosphorus, NaCl (100 mM), EDTA (0.1 mM), pH 7.0) by using 1.0 μM concentrations of each strand (see the Supporting Information for absolute T_m values.). [b] Differences in melting temperatures as compared to singly modified duplexes; $\Delta\Delta T_{m(x:y)} = \Delta T_{m(x:y)} - (\Delta T_{m(x:T2)} + \Delta T_{m(T1:y)})$. [c] Data taken from ref. [5].

lisation of the duplexes as compared to the unmodified DNA, and the thermal penalty paid for introducing 5′-substituents increased in the order **M** < **L** < **K** ≈ **N** < **O** ≈ **P**.

When the modified ONs were mixed to form duplexes with modifications in both strands, the possibility of zipper structures could be investigated. In the case of monomer **K** from our former study, a very selective (−3)-zipper contact was observed. Thus, when comparing entries 7, 8 and 10, in which the modifications are interspaced in the duplexes by none, one or three base pairs (defined as (−1)-, (−2)- and (−4)-zippers, respectively) a similar decrease in duplex stability of −9.8 to −10.4 °C was seen (Table 1). This corresponds roughly to the sum of two monosubstituted duplexes, and the $\Delta\Delta T_m$ values (corresponding to the deviation from a simple addition of the decreases obtained from the two corresponding monosubstituted duplexes) were in these cases <1 °C. On the other hand, entry 9 demonstrated that with the two modifications in a (−3)-zipper position, the duplex is more thermally stable than either of the two duplexes with just one modification (compare with entries 1 and 5), and the compensation with a $\Delta\Delta T_m = +6.5$ °C indicated an energetically favourable contact between the thymine moieties in the minor groove. When comparing entries 11–15 it was clear that this compensation is seen in all duplexes with two additional thymines (**K**) in (−3)-zipper orientations (entries 12, 13 and 15, $\Delta\Delta T_m$ values between +6.1 and +7.0 °C), whereas a constant thermal penalty around −6 °C for each monomer **K** is generally observed.

When the same zipper structures were studied with the monomer **L**, the decreases in duplex stability observed were in general within those obtained from just the addition of the decreases with only one modified strand, that is, ΔT_m values between −2.6 to −5.4 °C for each monomer and only small $\Delta\Delta T_m$ values reaching a maximum of +2.2 °C (entry 8). This shows that minor groove contacts are unlikely to occur. For monomer **M**, which generally showed the smallest decreases in duplex stability with single incorporations, the decreases were even more uniform (maximal $\Delta\Delta T_m = +1.4$ °C) and absolutely no indications of zipper contacts could be seen. The same is valid for monomer **N**, although it was noted that the $\Delta\Delta T_m$ values are positive in all cases. Nevertheless, the compensation in thermal stability was too small in all cases to indicate any specific zipper contacts, and the generally small positive $\Delta\Delta T_m$ values probably indicate that the distortion of hydration is largest for the first incorporation of a hydrophobic entity in the minor groove.

The situation became slightly more complicated in the case of monomers **O** and **P**. In general, the many positive $\Delta\Delta T_m$ values could indicate some minor-groove contacts although no specific contacts like the (−3)-zipper found for **K** were indicated. The most interesting results were obtained with monomer **O**, for example, by comparing the duplex with two monomers in the same strand (entry 3) with the duplexes formed when either one or two of the same monomer **O** was introduced in the complementary strand (entries 11 and 15, respectively). In this case the relatively unstable duplex ($\Delta T_m = -16.3$ °C) was significantly stabilised by 5–7 °C with the additional nucleobases in the minor groove (up to ΔT_m of −9.6 and −11.4 °C). This certainly indicates contacts in the minor groove, but again it does not seem to be specific for certain positions like the (−3)-zipper for **K**. All zipper possibilities between (+1) and (−4) are present in these duplexes. Concerning the duplexes with only one potential zipper contact (entries 7–10), a (−2)-zipper might be indicated, as the decrease in duplex stability was significantly smaller than for one of the single incorporation (ΔT_m of −4.4 as compared to −9.4, entry 2). On the other hand, when comparing with the other single incorporation ($\Delta T_m = -1.6$, entry 4), the second additional uracil has a negative effect and a general conclusion is not possible. For monomer **P**, some large positive $\Delta\Delta T_m$ values were observed (e.g., entries 11 and 12); this indicates a similar but somewhat weaker range of minor-groove contacts. In general, the duplexes containing monomer **P** were the least stable in the series. The only exceptions were entries 7 and 12, in which monomer **O** led to even further decreases in stability, and entries 8 and 11, for which monomer **K** revealed the least stable duplexes. This further confirmed that only monomer **K** formed the very specific (−3)-zipper contact and no other contacts.

From the results in Table 1, many indications of aromatic minor-groove contacts were indicated, but it is also clear that only the (−3)-zipper has been obtained specifically and only for monomer **K**. We decided to investigate whether this contact is dependent on the sequence context or on the bottom surface of the minor groove. As the interspacing sequence in our (−3)-zippers (entry 9, Table 1) is palindromic (TA:AT), it was only necessary to vary one of the two interspacing base pairs (Table 2). The study showed that regardless of sequence, the (−3)-zipper motif gave rise to a favourable interaction. However, there were differences in the magnitude of the stabilisation. Whereas, the original (−3)-zipper displayed an increase in T_m of +6.5 °C, the duplex with a reversed T:A base pair was slightly more stable ($\Delta\Delta T_m = +7.7$ °C). On the other hand, smaller relative stabilisations were obtained when a G:C or a C:G base pair was introduced in between the modifications ($\Delta\Delta T_m$ values of

Table 2. Sequence dependency for the (−3)-zipper motif with **K**.

Duplex **X**/**Y** =	T_m [°C][a] T/T	ΔT_m [°C][a] ($\Delta\Delta T_m$ [°C])[b] T/**K**	**K**/T	**K**/**K**
5′-d(CGC AT*A* **Y**TC GC) 3′-d(GCG **X**A*T* AAG CG)	46.7	−5.4	−4.9	−3.8 (+6.5)
5′-d(CGC AT*T* **Y**TC GC) 3′-d(GCG **X**A*A* AAG CG)	48.2	−4.0	−5.9	−2.2 (+7.7)
5′-d(CGC AT*G* **Y**TC GC) 3′-d(GCG **X**A*C* AAG CG)	51.3	−5.8	−4.5	−6.9 (+3.4)
5′-d(CGC AT*C* **Y**TC GC) 3′-d(GCG **X**A*G* AAG CG)	49.2	−3.6	−4.9	−4.9 (+3.6)

[a] See legend for Table 1; $\Delta T_{m(\mathbf{X}:\mathbf{Y})} = T_{m(\mathbf{X}:\mathbf{Y})} - T_{m(T:T)}$. [b] See legend for Table 1; $\Delta\Delta T_{m(\mathbf{K}:\mathbf{K})} = \Delta T_{m(\mathbf{K}:\mathbf{K})} - (\Delta T_{m(T:\mathbf{K})} + \Delta T_{m(\mathbf{K}:T)})$.

+3.4 and +3.6 °C). In other words, the stabilising effect of the (−3)-zipper thymine–thymine contact is somewhat dependent on the surface structure of the minor groove; this indicates a small negative effect of the protruding G:C base pair as compared to the A:T base pair.

To gain more insight on the nature of the (−3)-zippers we also investigated the duplexes formed by crossing the monomers of entry 9 (Table 1). Table 3 shows the hybridisation

Table 3. Crossed (−3)-zipper motifs of monomers **K**, **L**, **O** and **P**.[a]

5′-CGC ATA **Y**TC GC
3′-GCG **X**AT AAG CG
$\triangle T_m$ [°C] ($\triangle\triangle T_m$ [°C])

X\Y	T	**K**	**L**	**O**	**P**
T	0.0	−4.9	−4.5	−7.8	−7.5
K	−5.4	**−3.8 (+6.5)**	−1.2 (+8.6)	−11.4 (+1.8)	−9.1 (+3.8)
L	−3.2	−0.1 (+8.5)	**−6.3 (+1.4)**	−7.4 (+3.6)	−8.0 (+2.7)
O	−7.7	−11.6 (+1.0)	−9.4 (+2.8)	**−10.7 (+4.8)**	−13.3 (+1.1)
P	−6.9	−9.1 (+2.5)	−9.0 (+2.4)	−13.7 (+1.0)	**−13.8 (+0.6)**

[a] See legend for Table 1. The values shown in bold correspond to entry 9, Table 1.

data for these duplexes involving the monomers that have indicated the ability of forming interstrand contacts, **K**, **L**, **O** and **P**. In most cases, the duplex stability was almost as expected from the additive effect of the monomers (i.e., small $\Delta\Delta T_m$ values). However, a very interesting relative stabilisation was observed for the crossed (−3)-zipper motifs **L**:**K** and **K**:**L** with a $\Delta\Delta T_m$ of +8.6 and +8.5 °C, respectively. Both these zipper motifs showed an overall stability comparable to that of the unmodified duplex. In other words, the thymine–phenyl contacts in the minor groove are thermally stronger than the thymine–thymine contacts.

CD spectroscopy: CD spectra were recorded to gain global structural information on the modified duplexes. DNA duplexes preferentially adopt a B-form in solution, and these give characteristic CD spectra with a negative band at around 250 nm and a positive band at about 280 nm with almost equal magnitude.[20] The unmodified duplex of this study (represented as TT in Figure 1) demonstrated the expected B-type characteristics. CD of the duplexes with single incorporations of **K**, **L**, **O** and **P** (entries 1 and 5, Table 1) demonstrated spectra similar to that of the unmodified duplex (see the Supporting Information). For the (−3)-zippers (Table 3), small variations were seen (Figure 1). In general, the bands at about 250 and 280 nm tend to have a slightly lower amplitude, but also a few other changes were observed. The duplex with a (−3) **K**:**K** zipper showed a slightly different spectrum with a shift of the positive band towards 265 instead of 280 nm. The two crossed (−3)-zippers **L**:**K** and **K**:**L** showed identical trends. This follows the tendency from the melting temperatures (Table 3), and indicates that only these three duplexes have substantial interactions between the aromatic moieties in the minor groove. On the other hand, the duplex with a (−3) **O**:**O** zipper also

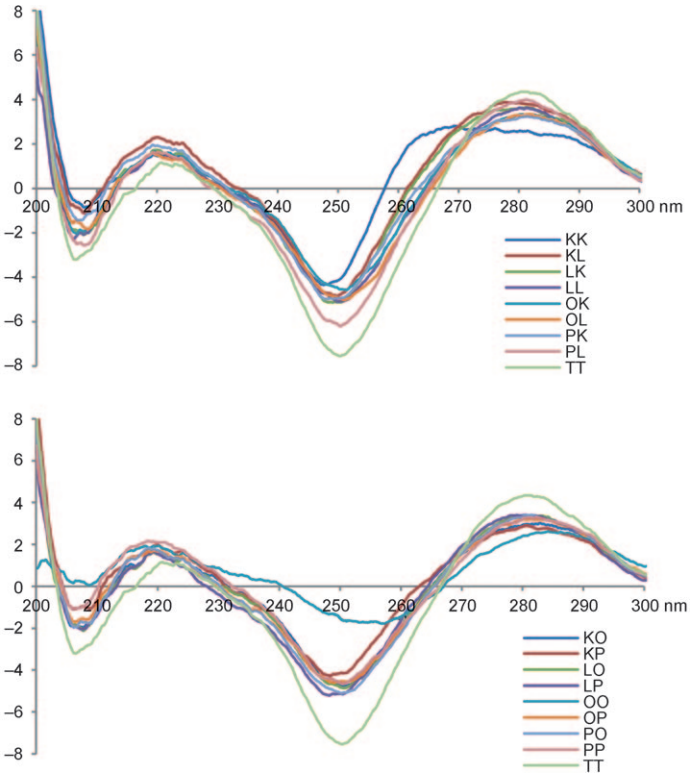

Figure 1. CD spectra of (−3)-zipper duplexes. The labelling "XY" corresponds to the sequences (X\Y) in Table 3.

exhibited a somewhat different spectrum with a much less intense negative band at 250 nm and a positive shoulder at 240 nm. This indicates that this duplex might deviate slightly from B-type geometry.

CD spectra were also recorded for some other duplexes (see the Supporting Information). In general there was little difference between the spectra of the modified duplexes and that of the unmodified duplex; this indicates that the introduction of the minor-groove-based units leaves the duplex structure fairly unaltered. In one case, however, notable differences were observed. This was for the (+1)-(−3)-"multi-zipper" of **O** (entry 15, Table 1). This duplex displayed a CD spectrum with a considerably larger negative band at about 250 nm and a larger positive band shifted towards 290 nm. This might indicate a change from B-type duplex geometry with four incorporations of **O**.

Molecular modelling: MD simulations were applied to enlighten two central observations: the increased (−3)-zipper contact between monomers **K** and **L** (Table 3), and the special behaviour of monomer **O** in various duplexes (Table 1). In accordance with the CD spectra of the modified duplexes (Figure 1 and the Supporting Information) we built all modified duplexes with an initial B-type duplex geometry. The duplexes all remained in a B-like geometry over the course of the 30 ns simulation, and base pairing was preserved for all base pairs throughout the simulations except for terminal base pairs for which some end-fraying was observed.

We have previously investigated the (−3)-zipper motif with monomer **K** and found that the two thymine bases are located in the minor groove and stack with each other.[5] In this study, we extended the study of minor-groove stacking by investigating the phenyl-substituted analogue, **L**. We carried out 30 ns MD simulations for the four combinations of **K** and **L** (Table 3). In all simulation, the aromatic rings spontaneously stacked with each other during the entire simulation although there were variations between the tightness and mode of stacking. In the **K**:**K** duplex, the hydrophilic edge of the thymine was directed towards the solvent while the hydrophobic edge with the methyl group pointed towards the bottom of the minor groove. The stacking interaction changed little over the course of the simulation with the two aromatic rings being about 3.6 Å apart and positioned almost right on top of each other similar to the depiction shown in Figure 2a. This arrangement fits seamlessly into the minor groove with the methyl groups making van der Waals contacts with the opposite walls of the groove. The cross-groove stacking interaction locks the sugar–phosphate backbone locally and the ε/ζ angles adjacent to the modified C5′ are exclusively found with a B_I ($\varepsilon \approx 180°$, $\zeta \approx -90°$) conformation whereas all other nucleotides attain both the B_I and B_{II} ($\varepsilon \approx -100°$, $\zeta \approx 170°$) conformations during the simulation. Apart from this minor change, the local geometry is virtually left unaltered by the inclusion and stacking of the additional thymine bases.

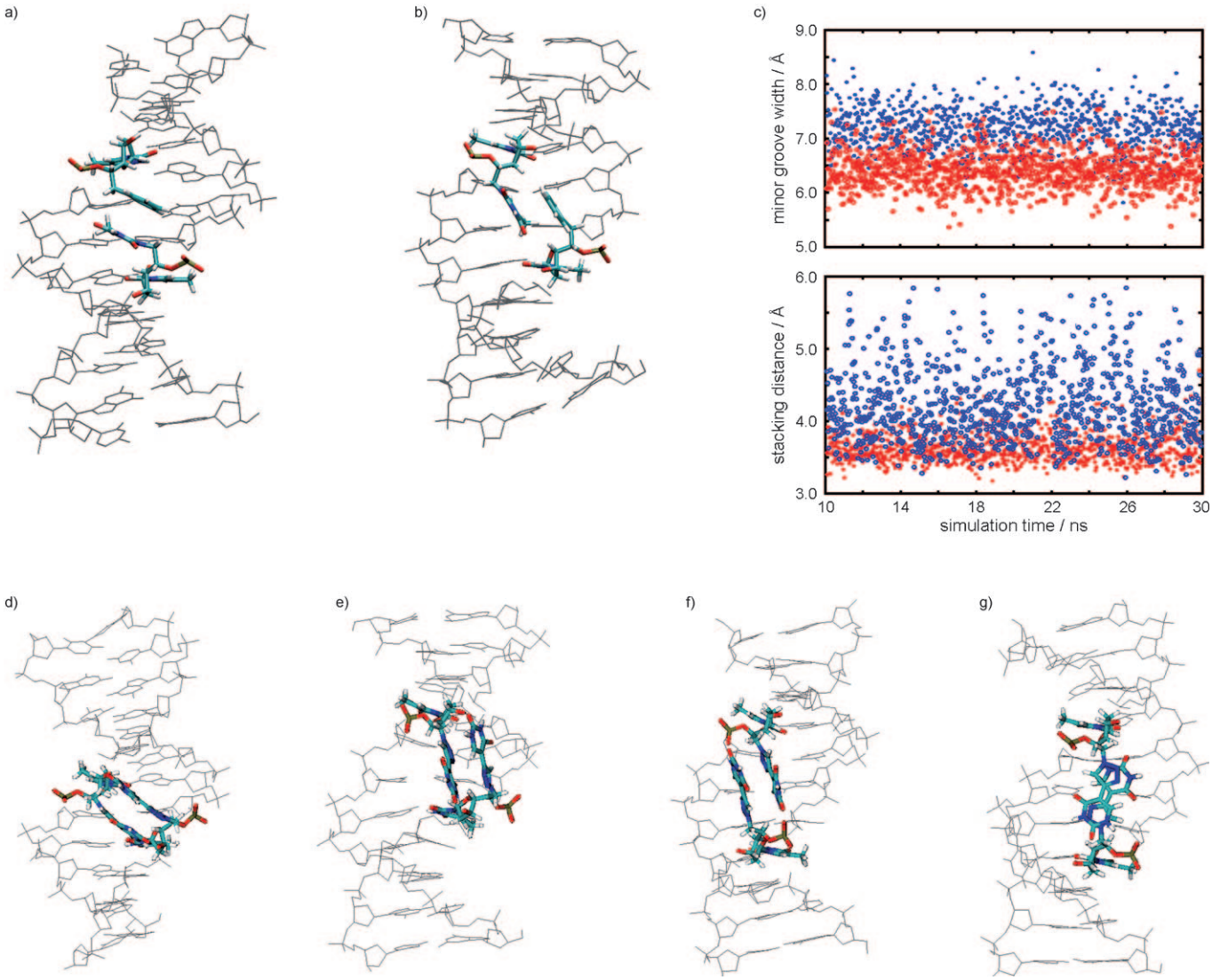

Figure 2. a), b) Snapshots of the two stacking motifs observed for the thymine and phenyl moieties in the minor groove. A) The motif giving the best overlap of π electron systems, and b) the "cross-over" motif. The duplexes shown are: a) the (−3) **K**:**L** zipper, and b) the (−3) **L**:**K** zipper (Table 3). c) The minor-groove width across the stacking site of the **K**:**K** (blue) and **K**:**L** (red) zipper duplexes and the stacking distance between the minor groove located aromatic moieties of the **K**:**L** (red) and **L**:**L** (blue) duplexes. The minor groove width was measured as the interstrand phosphorus distance minus the van der Waals radii of the phosphate groups, and the stacking distance was determined as the distance between the geometric centres of the six-membered rings. d)–g) Snapshots of various **O**:**O** zipper motifs. d) The (−2)-zipper (entry 8, Table 1); e) the (−3)-zipper (entry 9, Table 1); and f) the (−4)-zipper (entry 10, Table 1); g) the (−4)-zipper motif in which one **O** unit is hydrogen bonded to the (−3)-adenine N3 atom while the other **O** unit stacks onto the first one. The snapshot is from the simulation of entry 11, Table 1.

An alternative stacking arrangement, in which the two thymines were reversed, were also observed in our simulations as shown in Figure 2b. In this arrangement, the linker from C5′ crossed the edge of the thymine base from the complementary strand and hence the two thymine bases cannot reach fully across each other, which probably diminished their stacking interaction (see below).

A very similar stacking arrangement as in the **K**:**K** duplex was observed with **K**:**L**, but the minor groove was narrowed by about 1 Å (Figure 2c) and consequently the two aromatic moieties filled the void of the groove even better in this case than in the **K**:**K** duplex (Figure 2a). In the **L**:**K** duplex, the phenyl and thymine moieties at first stacked in the cross-over manner (Figure 2b) but after about 8 ns this interaction was broken and a stacking motif following the pattern in Figure 2a was created. It thus seems that this arrangement is the more stable of the two. However, as opposed to both the **K**:**K** and **K**:**L** duplexes, the hydrophilic edge of the thymine was turned towards the bottom of the groove while the hydrophobic edge with the methyl group was oriented towards the solvent. Although this stacking arrangement in principle should allow for as good a stacking between the phenyl and thymine moieties as when the thymine is rotated 180°, we observed several instances in which the stacking was disrupted temporarily while either the phenyl or the thymine moved into the solvent. As such, this orientation of the thymine base seems not to produce the optimum cross-strand interaction with the phenyl.

One can speculate as to why the **K**:**L** and **L**:**K** duplexes display a higher thermostability than the **K**:**K**. One unfavourable aspect of the thymine stacking in the **K**:**K** duplex is that the dipole moments of the thymine bases are almost co-aligned with each other and the two carbonyl groups are nearly on top of one another. Unfavourable factors for the **K**:**L** and **L**:**K** duplexes are the lower polarisability of the phenyl group compared to thymine, the lack of the methyl group to make van der Waals contacts with the groove wall, and the lack of a hydrophilic edge to partake in water interactions. From the melting temperature data, we can conclude that the unfavourable electrostatic interactions outweigh the detrimental factors when a thymine is replaced with a phenyl. It is perhaps particularly interesting to note that the loss of hydrogen bonding capabilities are more than counteracted by not having repulsive dipoles. The balance between having a thymine or a phenyl group is finely tuned, however, as is evident from the melting temperature of the **L**:**L** duplex, which melts at a temperature 5–6 °C lower than **K**:**L** and **L**:**K**. In our simulation of the **L**:**L** duplex, the two phenyl groups stacked in the minor groove, but the stacking was markedly less tight than that of thymine–thymine and thymine–phenyl with both phenyl groups being rather dynamic and stacking interactions often being broken and reformed (Figure 2c).

To investigate the molecular basis for the behaviour of the 5′ connected uracil-triazole moiety of **O**, we also conducted MD simulations of all duplexes containing **O** (entries 1–15, Table 1). The triazole moiety was assigned atom types from the generalised Amber force field (GAFF) and the uracil bases were assigned types from the Amber99SB force field. Where needed force field parameters combining interactions between GAFF and Amber99SB atom types were deduced by atom type analogy. In an earlier study, the torsion profile for rotation between uracil and triazole moieties in a similar arrangement was determined by MP2/6-31G* ab initio calculations.[19] A deep minimum around the coplanar conformation with the CH of the triazole and the O4 of the uracil in close proximity was found.[19] The force field parameters did not reproduce the ab initio profile but rather yielded two minima for this rotation, one each when the two aromatic rings were coplanar. Therefore, the uracil-triazole force field torsion profile was fitted to reproduce the ab initio profile and thereby the uracil and triazole moieties were placed in the favoured geometry (Figure S3 in the Supporting Information). In the starting structures for simulations, the uracil-triazole unit was placed pointing into the solvent so as not to bias any type of interaction. In all cases, the uracil-triazole unit engaged in interactions with the remainder of the duplex at some stage of the simulation.

At first we established the different types of interactions between the uracil-triazole unit and the double stranded DNA (dsDNA) by analysis of the duplexes with a single modification (entries 1, 2, 4 and 5, Table 1). In all cases hydrogen bonding between the NH groups of the uracil and phosphate groups in the complementary strand was observed, and was found to occur in three alternative manners across the minor groove (Figure S4 in the Supporting Information). Two different phosphate groups are targeted, the (−3) and (−4) groups (i.e., the phosphate groups 3 and 4 positions away, respectively, in the 3′ direction in the complementary strand). When hydrogen bonding to the (−3)-phosphate group, the uracil-triazole unit is placed almost parallel with the base pairs and makes an average angle of around 25° with the C1′-C1’ vector of the neighbouring base pair. The uracil-triazole unit is located with the hydrophobic large π electron system presented towards the solvent. For hydrogen bond formation with the (−4)-phosphate group, a rotation of about 45° of the uracil-triazole unit is needed relative to the (−3)-phosphate hydrogen bond. In both these types of interactions, the uracil-triazole unit lies like a lid across the minor groove and probably disturbs the minor groove hydration heavily. With these types of interactions, the minor groove was narrowed locally in the range of up to around 1 Å. For the hydrogen bonding to the (−4)-phosphate group a second motif was observed, in which the uracil-triazole unit was rotated further and ran almost along the minor groove. There appears to be no preference for either binding motif as they are all substantially populated in the simulations although different duplexes show different preferences.

It is interesting to compare the melting temperatures of duplexes modified with monomers **O** and **P**. Because the size of the uracil-triazole and phenyl-triazole units is similar, the difference is in their hydrogen bond capabilities. In general the two modifications are tolerated either equally well

or bad in a duplex context when one modification is present (Table 1). This appears to show that the interstrand hydrogen bonding is of little or no importance in terms of thermostability. The conspicuous exception is entry 4, in which a remarkable relative stabilisation was obtained with **O** as compared to **P**. In our simulations, a short-lived hydrogen bond from the uracil to the (−3)-adenine N3 at the bottom of the minor groove was observed; this was the only feature to distinguish this duplex from the others.

We next examined duplexes possessing two **O** monomers in separate strands allowing for zipper interactions (entries 7–10, Table 1). Comparing melting temperatures for these duplexes, it is apparent that whereas a penalty corresponding almost fully to introduction of two monomers of **O** in the same strand was observed for the (−1)-zipper (entry 7), much smaller penalties were paid for introduction of two **O** monomers in (−2)-, (−3)- and (−4)-zippers (entry 8–10). In the simulations of the (−1)-zipper, we observed hydrogen bonding to both the (−3)- and (−4)-phosphates of the complementary strand for both uracil-triazole units with concomitant narrowing of the minor groove to approximately 5 Å. These interstrand interactions were basically uncorrelated. The (−2)-zipper motif of **O** showed a decrease in melting temperature of only 4.4 °C compared to the unmodified DNA duplex; this indicates a considerable gain in stability by the inclusion of two **O** modifications. In the simulation, both uracil-triazole units hydrogen bonded to the (−4)-phosphates on and off during the early part of the simulation. After approximately 14 ns, they concurrently switched to bind to the (−3)-phosphate groups and started stacking with each other (Figure 2d). In particular the uracil-triazole unit of the O2 strand displayed some mobility and in between abolished hydrogen bonding and rotated slightly towards the bulk solvent. During the periods of tightest stacking, the two uracil-triazole units form an angle of about 120° with each other. The cross-strand hydrogen bonding and stacking of the two uracil-triazole units caused the minor groove to be narrowed by about 1 Å. In the (−3)-zipper motif of **O** (entry 9, Table 1), the two uracil-triazole units propelled into a hydrogen bonding and stacking mode after around 3 ns of simulation and remained so during the remainder of the simulation (Figure 2e), which shows that the (−3)-zipper positions of the uracil-triazole units is favourable for interstrand interactions. Both uracil-triazole units hydrogen bonded to the (−4)-phosphate group of the complementary strand and their stacking was associated with a uracil-triazole unit–unit angle of about 120–130°. The continuous hydrogen bonding and stacking across the minor groove narrowed it by 1.5–2.0 to approximately 5.2 Å on average throughout the centre of the duplex. In the (−4)-zipper motif of **O** (entry 10) we again observed tight and prolonged stacking between the two uracil-triazole units from about 7 ns and onwards in the simulation. The preferred hydrogen bond option was again the (−4)-phosphate groups although the altered position of the uracil-triazole units precluded continuous hydrogen bonding for both uracil moieties. Consequently, two different stacking geometries were observed with the most populated one shown in Figure 2f. Both geometries had an inter-uracil-triazole angle of about 100–120° in common.

Taken together, it is clear that the uracil-triazole units are able to interact for prolonged periods when placed in (−2)-, (−3)- and (−4)-zippers, which account for their increased thermostability compared to the (−1)-zipper. It is noteworthy that the (−2)-zipper motif also yields the best thermostability in the case of monomer **P**. This points to preferred stacking interactions in this zipper as compared to the other zippers.

For the duplexes with three **O** monomers incorporated (entries 11–14, Table 1) the first is conspicuous both in the **O** series and when compared with the **P**-modified duplexes. In this duplex (entry 11) interstrand stacking was observed throughout the simulation after around 3 ns. At first the (−4)-positioned uracil-triazole units stacked upon each other in a manner similar to that observed in the (−4)-zipper duplex (entry 10). After about 19 ns the uracil-triazole unit of sequence O4 rotated and stacked with the (−2)-positioned uracil-triazole unit in a fashion similar to entry 8. This interaction persisted for about 3 ns, after which the uracil-triazole unit of sequence O4 rotated into the bottom of the minor groove and made a hydrogen bond with the N3 nitrogen of the (−3)-adenine. This interaction persisted on and off for the remainder of the simulation (~8 ns). While the uracil-triazole unit of sequence O4 hydrogen bonded to the bottom of the minor groove, the (−4)-positioned uracil-triazole unit stacked on top of it with the two units making an angle of about 160° with each other (Figure 2g). Although this type of interaction would also be possible in the (−4)-zipper duplex (entry 10), we did not observe it during our simulation. This might be a consequence of insufficient sampling of conformational space even though the simulation was extended to 30 ns. The penalty in thermostability for incorporating three **O** monomers is in general greater than the penalty paid for two monomers. This concurs with our simulations and shows that at no time more than two of the uracil-triazole units can interact with each other.

The multizipper motif (entry 15, Table 1) possessing four monomers of **O** is noteworthy as the thermostability of this duplex is higher than that of the triple modified duplexes (entries 12–14) and on par with that of the (−3)-zipper duplex (entry 9). Thus incorporation of an additional modification confers added stability and the addition of two extra modifications are tolerated by the (−3)-zipper duplex. These results are intriguing, but our simulation did not shed light on this phenomenon. The two (−3)-positioned uracil-triazole units stacked with each other while the two others crossed the minor groove as observed in the single-modified duplexes. Because the CD spectrum of this duplex (see the Supporting Information) was somewhat anomalous, we carried out a further simulation of this duplex initiated from an A-type geometry. However, this simulation also led to a B-type geometry with the two distant uracil-triazole units stacking again.

Discussion

The present study demonstrates that the 5′-(*S*)-*C*-position is excellent for placing aromatic moieties into the minor groove of DNA duplexes. The synthesis of various monomers is relatively straightforward, and from a common 5′-azidomethyl group a range of substituted triazoles can be easily obtained by the CuAAC reaction. Concerning the thermal stability of the resulting duplexes, a penalty is paid in all cases, probably due to a combination of slight sterical disturbance and a distortion of the duplex hydration. Small 5′-*C*-substituents, like methyl, hydroxymethyl and others, have earlier demonstrated relatively small but unavoidable decreases in duplex stabilities (ΔT_m values of 1–3 °C for each incorporation),[21–23] and these thermal penalties seem to increase with the sterical bulk of the substituent. Leumann and co-workers inserted hydrophobic butyl and isopentyl substituents and observed decreases of around 2–3 °C.[24] In this study decreases in thermostability generally ranged between 1 and 3.5 °C for each small **M** monomer to between 6 and 9 °C for each of the larger and more hydrophobic **P** monomers. On the other hand, the studies of zippers clearly demonstrate that these thermal penalties can be partly compensated for by minor-groove contacts between various substituents either by stacking across the minor groove or hydrogen bonding to phosphate groups of the opposite strand or to the bottom of the groove.

The most fundamental and selective zipper contact is the (−3)-zipper as found for two thymines in the minor groove inserted by two **K** monomers. Even a change of the minor groove surface below the zipper contact only slightly distorted the contact. In this study, we have explored the (−3)-zipper motif, and interestingly the zipper contact improved with a crossed (−3)-zipper between a thymine and a phenyl group (combining **K** with **L**). With this contact the native duplex thermostability is retained despite the introduction of two bulky 5′-substituents. The generality of the (−3)-zipper is shown by interchanging **K** and **L** (Table 3). The favourable (−3)-zipper is specific for combination of **K** and **L** as compared with the **K**:**K** and **L**:**L** zippers (Table 3). This is an interesting example of the subtle forces that govern stacking capabilities. Our modelling shows that the duplex with the **K**:**L** zipper is more compact than that with the **K**:**K** zipper. The interaction site in the **K**:**L** zipper is symmetric so it is not steric repulsion by the slightly larger thymine that causes the slight widening of the minor groove in the **K**:**K** zipper. Hence, it appears likely that the difference is a consequence of improved **K**:**L** stacking as compared with **K**:**K** stacking, which is somewhat surprising given the larger electron cloud of thymine. However, the modelling shows that if two thymines should adopt the same stacking pattern as a thymine and a phenyl, then the carbonyl and imino moieties would be very close to exactly on top of each other leading to a slight electrostatic repulsion. On the other hand, the **L**:**L** zipper is less stable than both **K**:**K** and **K**:**L** zippers. Our modelling shows that in the **L**:**L** zipper, the two phenyl rings are mobile and move around in the minor groove and hence do not create the tight stacking contacts observed for the **K**:**K** and **K**:**L** zippers. Thus, it seems that the extra stacking capability of a thymine is needed to ensure tight stacking or that the loss of both hydrophilic edges of thymines disturbs the interaction with water too extensively.

It is clear from the modelling that the six-membered rings of thymine or phenyl fit snugly into the minor groove and reach perfectly across it to interact with the opposite groove wall. Hence, it is of no surprise that no other very favourable (−3)-zippers are obtained when including either monomer **M**, **N**, **O** or **P** as these moieties are either too small or too large to be accommodated in the minor groove in the same manner as monomer **K** or **L** (Tables 1 and 3). While no specific favourable contacts are observed for the smaller aromatic systems of **M** and **N**, it is still conspicuous that in general **M** is accommodated better in duplexes. This shows that the hydrogen bond donating ability of **M** is important. This correlates with the hydrogen bonding ability of thymine possibly being important for the **K**:**L** (−3)-zipper motif.

For the larger aromatic systems of **O** and **P**, the results are not systematic. This is supported by the modelling studies as a wide range of different contacts across the minor groove were observed for monomer **O**. The modelling of all duplexes incorporating one to four monomers of **O**, however, have demonstrated the dynamic potential in using a relatively complicated substituent like uracil-triazole with a multitude of binding possibilities for designing minor-groove communication. Hence, in one sequence (entry 4, Table 1), the binding to an adenine might give a relative increase in T_m of around 5 °C, and in another (the (−2)-zipper motif, entry 8), the stacking of the substituents gives a similar thermal compensation. In the multizipper motif (entry 15) the complicated interactions of four substituents might change the overall duplex structure as indicated in the CD spectrum. Our modelling did not capture such a change of structure, which might be a consequence of incomplete sampling.

Recently, Leumann and co-workers have shown that biphenyl and cyclohexyl-phenyl units can be accommodated in the centre of a dsDNA duplex where they partake in the Watson–Crick ladder of stacking.[25] The biphenyl and cyclohexyl-phenyl units were attached to the deoxyribose sugar at the C1′ carbon as a replacement for the natural nucleobase. In this study, we extend the accommodation of bicyclic aromatic ring systems from the centre of the duplex to the edge of the duplex in the minor groove. The accommodation of the large aromatic systems in the minor groove is unfavourable for duplex thermostability but we show that the penalty paid can be kept down by judicious positioning of **O** or **P** monomers.

To extend our studies, it would be interesting to study how more densely modified duplexes would behave. Leumann and co-workers have pursued this line of work with their hydrophobic alkyl 5′-substituted analogues. The substituted monomers were placed as either consecutive or alternating incorporations.[24] The decrease in thermal duplex stability was remarkably unchanged irrespective of the arrange-

ment of substituents. This indicates that their main effect is distortion of the hydration pattern rather than any kind of intersubstituent communication. We may speculate that aromatic and hydrophilic substituents like those of the present study would behave differently either being better accepted in the duplex hydration pattern or sterically filling the minor groove to a larger extent and adding to the thermal stability by efficient stacking and van der Waals interactions with the groove walls. While the interactions with the **O** and **P** monomers in multiples are difficult to predict, it seems fairly straightforward from our molecular models that **K** and/or **L** monomers can be accommodated in a continuous manner through the minor groove of a B-type dsDNA. Future studies will demonstrate the scope of decorating the DNA duplex in the minor groove.

Overall, we have demonstrated that communication between the complementary strands in a DNA duplex can be obtained in the minor groove parallel with the Watson–Crick base pairing in the duplex core, and thus extend the structural space available for equipping the Watson–Crick duplex with functional units. Such decoration of a DNA duplex can be important for DNA-based self-assembling nanomaterials.

Conclusion

Easy synthesis has led to subtle and specific decoration of the DNA duplex with aromatic moieties in the minor groove. The aromatic units communicate in or across the minor grove without any violation of the duplex structure or the central Watson–Crick base pairing. The strongest and most selective stacking interaction was found between a thymine and a phenyl moiety in a (−3)-zipper orientation. Hence, with our work we have incremented knowledge of the Watson–Crick duplex as a scaffold for delicate organisation of functional moieties. Furthermore, the present study adds to the knowledge on the dynamic behaviour of decorated DNA duplexes.

Experimental Section

General: All commercial reagents were used as supplied. Reactions were carried out under argon or nitrogen when anhydrous solvents were used. Column chromatography was performed with Silica gel 60 (particle size 0.040–0.063 μm; Merck). NMR spectra were recorded on a Varian Gemini 2000 spectrometer or a Bruker Advance III 400 spectrometer. Values for δ are given in ppm relative to tetramethylsilane as an internal standard or H_3PO_4 (85%) as an external standard. Assignments of NMR signals when given are based on 2D spectra and follow standard nucleoside convention. ESI mass spectra as well as accurate mass determinations were performed on a Thermo Finnigan TSQ 700 spectrometer. Microwave heated reactions were performed with an Emrys™ Creator.

Synthesis of 5′-(*S*)-*C*-benzyl-3′-*O*-(*tert*-butyldimethylsilyl)-5′-*O*-pixylthymidine (7): A suspension of CuI (157 mg, 0.82 mmol) in anhydrous THF (75 mL) was stirred at −78 °C and a solution of PhMgBr (1 M) in THF (16.5 mL, 16.5 mmol) was added. A solution of epoxide **6** (582 mg, 1.58 mmol) in anhydrous THF (15 mL) was added, and the mixture was stirred at room temperature for 90 min. A saturated aqueous solution of NH_4Cl (50 mL) was added. The mixture was extracted with CH_2Cl_2 (3× 50 mL) and the combined organic phase was washed with water (50 mL), dried ($MgSO_4$) and concentrated under reduced pressure. The residue was purified by column chromatography (0–10% EtOH in $CHCl_3$) to give the crude intermediate as a white foam; $R_f = 0.3$ (CH_2Cl_2/MeOH, 95:5, v/v); HRMS (ESI): *m/z*: calcd for $C_{23}H_{34}N_2O_5SiNa^+$ $[M+Na]^+$: 469.2129; found: 469.2111. The intermediate was coevaporated with anhydrous pyridine and dissolved in the same solvent (14 mL). Pixyl chloride (1.15 g, 3.91 mmol) was added and the mixture was stirred at room temperature for 20 h. The mixture was concentrated under reduced pressure and coevaporated twice with a mixture of toluene and ethanol (1:1, v/v). The residue was redissolved in CH_2Cl_2 (35 mL) and washed with a saturated aqueous solution of $NaHCO_3$ (25 mL) and water (2×25 mL). The aqueous phase was extracted with CH_2Cl_2 (2×25 mL), and the combined organic phase was dried ($MgSO_4$) and concentrated under reduced pressure. The residue was purified by column chromatography (0–40% EtOAc in petrol ether) to give product **7** as a white foam (524 mg, 47%). $R_f = 0.7$ (petrolether/EtOAc, 30:70, v/v); ^{1}H NMR (300 MHz, $CDCl_3$): $\delta = 8.73$ (br s, 1H; NH), 7.98 (s, 1H; H-6), 7.50–6.71 (m, 18H; Ph, pixyl), 6.22 (m, 1H; H-1′), 3.43–3.33 (m, 2H; H-4′, H-5′), 3.17 (d, $J = 3.2$ Hz, 1H; H-3′), 2.72 (t, $J = 12.6$ Hz, 1H; H-6′), 2.11–1.93 (m, 5H; H-2′, H-6′, CH_3(T)), 1.75 (m, 1H; H-2′), 0.58 (s, 9H; $C(CH_3)_3$), −0.31 (s, 3H; $SiCH_3$), −0.51 ppm (s, 3H; $SiCH_3$); ^{13}C NMR (75 MHz, $CDCl_3$): $\delta = 163.9$ (C-4), 152.3, 150.3, 147.0, 137.5, (C-2, pixyl), 136.3 (C-6), 132.1, 130.8, 130.4, 129.4, 128.5, 128.0, 127.7, 127.5, 126.3, 124.0, 123.8, 123.4, 116.9 (Ph, pixyl), 110.7 (C-5), 87.3 (C-4′), 85.4 (C-1′), 77.9 (pixyl), 75.9 (C-5′), 74.5 (C-3′), 41.4 (C-2′), 38.7 (C-6′), 25.8 ($C(CH_3)_3$), 17.8 ($C(CH_3)_3$), 12.9 (CH_3(T)), −4.8, −5.1 ppm (CH_3Si); HRMS (ESI): *m/z*: calcd for $C_{42}H_{46}N_2O_6SiNa^+$ $[M+Na]^+$: 725.3018; found: 725.3001.

Synthesis of 5′-(*S*)-*C*-benzyl-5′-*O*-pixylthymidine (8): A solution of TBAF (1.0 M) in THF (0.27 mL, 0.27 mmol) was added to a stirred solution of nucleoside **8** (190 mg, 0.27 mmol) in anhydrous THF (3 mL). The solution was stirred at room temperature for 20 h and then CH_2Cl_2 (5 mL) was added. The mixture was washed with an aqueous solution of $NaHCO_3$ (0.2 M; 10 mL), and the aqueous phase was extracted with CH_2Cl_2 (2×5 mL). The combined organic phase was dried ($MgSO_4$) and concentrated under reduced pressure. The residue was filtered through silica (0.25% Et_3N in CH_2Cl_2) to give product **8** containing 0.5 equiv Et_3N as a white foam (148 mg, 86%). $R_f = 0.3$ (CH_2Cl_2/MeOH, 5:95, v/v); ^{1}H NMR (300 MHz, $CDCl_3$): $\delta = 7.81$ (s, 1H; H-6), 7.55–6.71 (m, 18H; Ph, pixyl), 6.21 (t, $J = 6.8$ Hz, 1H; H-1′), 3.50–3.37 (m, 3H; H-3′, H-4′, H-5‘), 2.79 (t, $J = 11.4$ Hz, 1H; H-6′), 2.12–1.91 ppm (m, 6H; H-2′, H-6′, CH_3(T)); ^{13}C NMR (75 MHz, $CDCl_3$): $\delta = 164.3$ (C-4), 152.2, 150.6, 147.0 (C-2, pixyl), 137.4 (C-6), 135.9, 132.1, 130.9, 130.3, 130.0, 129.6, 128.5, 128.0, 127.9, 127.4, 126.3, 124.1, 123.7, 123.4, 116.8 (Ph, pixyl), 110.9 (C-5), 85.6 (C-4′), 84.4 (C-1′), 77.6 (pixyl), 74.7 (C-3′), 71.2 (C-5′), 40.7 (C-2′), 38.6 (C-6′), 13.0 ppm (CH_3(T)); HRMS (ESI): *m/z*: calcd for $C_{36}H_{33}N_2O_6Na^+$ $[M+Na]^+$: 611.2153; found: 611.2135.

Synthesis of 5′-(*S*)-*C*-benzyl-3′-*O*-(*P*-2-cyanoethyoxy-*N*,*N*-diisopropylaminophosphinyl)-5′-*O*-pixylthymidine (9): *N*,*N*-Diisopropylethylamine (1.4 mL) and *N*,*N*-diisopropylamino-2-cyanoethylphosphinochlorite (0.25 mL, 1.12 mmol) were added to a stirred solution of nucleoside **8** (369 mg, 0.63 mmol) in anhydrous 1,2-dichloroethane (7 mL). The solution was stirred at room temperature for 2.5 h. Ethanol (2 mL) was added and the solution was diluted with CH_2Cl_2 (15 mL) and washed with a saturated aqueous solution of $NaHCO_3$ (25 mL). The aqueous phase was extracted with CH_2Cl_2 (2×15 mL), and the combined organic phase was dried ($MgSO_4$) and concentrated under reduced pressure. The residue was purified by column chromatography (0–40% EtOAc in petrol ether) and the residue was precipitated from EtOAc/petrol ether to give product **9** as a white foam, which was approximately 75% pure but was used without further purification in the ON synthesis (232 mg, ≈39%). $R_f = 0.6$ (petrol ether/EtOAc, 30:70, v/v); ^{31}P NMR (300 MHz, $CDCl_3$): $\delta = 152.1$, 151.2; HRMS (ESI): *m/z*: calcd for $C_{45}H_{49}N_4O_7PNa^+$ $[M+Na]^+$: 811.3231; found: 811.3237.

Synthesis of 5′-(*S*)-*C*-azidomethyl-3′-*O*-(*tert*-butyldimethylsilyl)thymidine (10): NaN_3 (610 mg, 9.34 mmol) was added to a stirred solution of epox-

ide **6** (1.75 g, 4.74 mmol) in DMF (10 mL) and the mixture was stirred at 55 °C for 3 h. EtOAc (50 mL) was added and the mixture was washed with brine (50 mL), dried (Na_2SO_4) and concentrated under reduced pressure. The residue was coevaporated with xylene (10 mL) and toluene (10 mL) and purified by column chromatography (0–1 % MeOH in CH_2Cl_2) to give **10** as a white foam (1.65 g, 80 %); R_f = 0.49 (CH_2Cl_2/MeOH, 9:1, v/v); ^{1}H NMR (300 MHz, $CDCl_3$): δ = 8.81 (br s, 1H; NH), 7.37 (d, J = 0.9 Hz, 1H; H-6), 6.02 (t, J = 6.6 Hz, 1H; H-1′), 4.54 (m, 1H; H-3′), 3.87–3.82 (m, 2H; H-4′, H-5′), 3.53–3.35 (m, 2H; H-6′), 2.50 (m, 1H; H-2′), 2.15 (m, 1H; H-2′), 1.92 (d, J = 0.9 Hz, 3H; CH_3(T)), 0.89 (s, 9H; C(CH_3)$_3$), 0.08 ppm (s, 6H; Si(CH_3)$_2$); ^{13}C NMR (75 MHz, $CDCl_3$): δ = 163.8 (C-4), 150.5 (C-2), 138.0 (C-6), 111.3 (C-5), 88.9 (C-1′), 87.5 (C-4′), 73.0 (C-3′), 70.2 (C-5′), 54.4 (C-6′), 39.8 (C-2′), 25.8 (C(CH_3)$_3$), 18.0 (C(CH_3)$_3$), 12.6 (CH_3(T)), −4.4, −4.6 ppm (CH_3Si); IR: $\tilde{\nu}$ = 3429, 2954, 2929, 2858, 2105, 1694, 1472, 1277, 1121, 1049, 837, 779 cm^{-1}; HRMS (MALDI): m/z: calcd for $C_{17}H_{29}N_5O_5SiNa^+$ [M+Na]$^+$: 434.1830; found: 434.1819.

Synthesis of 5′-(*S*)-*C*-azidomethyl-3′-*O*-(*tert*-butyldimethylsilyl)-5′-*O*-pixyl-thymidine (11): DMAP (420 mg, 3.43 mmol) and pixyl chloride (1.02 g, 3.49 mmol) were added to a stirred solution of **10** (700 mg, 1.60 mmol) in MeCN (10 mL). The reaction mixture was stirred in a MW reactor at 120 °C for 30 min. EtOAc (35 mL) was added, and the mixture was washed with water (35 mL), dried (Na_2SO_4) and concentrated under reduced pressure. The residue was purified by column chromatography (2–5 % acetone in CH_2Cl_2) to give product **11** as a white foam (780 mg, 72 %) as well as the starting material (110 mg, 15 %). R_f = 0.38 (CH_2Cl_2/MeOH, 95:5, v/v); ^{1}H NMR (300 MHz, $CDCl_3$): δ = 8.64 (br s, 1H; NH), 7.67 (s, 1H; H-6), 7.47–7.26 (m, 9H; pixyl), 7.14–6.95 (m, 4H; pixyl), 6.20 (dd, J = 8.1, 13.9 Hz, 1H; H-1′), 3.80 (d, J = 2.4 Hz, 1H; H-4′), 3.55 (d, J = 6.9 Hz, 1H; H-3′), 3.35 (m, 1H; H-5′), 2.97 (dd, J = 13.2, 18.6 Hz, 1H; H-6′), 2.48 (dd, J = 5.4, 18.6 Hz, 1H; H-6′), 2.09–1.99 (m, 4H; H-2′, CH_3(T)), 1.85 (m, 1H; H-2′), 0.80 (s, 9H; C(CH_3)$_3$), −0.08 (s, 3H; CH_3), −0.13 ppm (s, 3H; CH_3); ^{13}C NMR (75 MHz, $CDCl_3$): δ = 163.8 (C-4), 151.9, 151.8, 150.2, 146.5 (pixyl, C-2), 135.8 (C-6), 131.4, 130.9, 130.4, 128.0, 127.5, 123.9, 123.1, 122.8, 117.1, 116.9 (pixyl), 110.8 (C-5), 87.8 (C-4′), 85.2 (C-1′), 78.2 (pixyl), 73.6 (C-3′), 71.7 (C-5′), 51.1 (C-6′), 41.0 (C-2′), 25.7 (C(CH_3)$_3$), 17.8 (C(CH_3)$_3$), 12.8 (CH_3(T)), −4.5, −4.7 ppm (CH_3Si); IR: $\tilde{\nu}$ = 3422, 2953, 2929, 2856, 2104, 1694, 1477, 1448, 1320, 1295, 1275, 1101, 1048, 836, 758 cm^{-1}; HRMS (ESI): m/z: calcd for $C_{36}H_{41}N_5O_6SiNa^+$ [M+Na]$^+$: 690.2719; found: 690.2723.

Synthesis of 3′-*O*-(*tert*-butyldimethylsilyl)-5′-(*S*)-*C*-(4-phenyl-1,2,3-triazol-1-yl)methyl-5′-*O*-pixylthymidine (12): Sodium ascorbate (37 mg, 0.37 mmol) and $CuSO_4$·5H_2O (25 mg, 0.052 mmol) were added to a stirred solution of compound **11** (500 mg, 0.75 mmol) and 1-phenylacetylene (114 μL, 1.08 mmol) in a mixture of THF, water and pyridine (10 mL, 3:1:1 v/v). The mixture was stirred at room temperature for 3 h and CH_2Cl_2 (30 mL) was added. The mixture was washed with water (30 mL), and the aqueous phase was extracted with CH_2Cl_2 (3×30 mL). The combined organic phase was dried (Na_2SO_4) and concentrated under reduced pressure. The residue was purified by column chromatography (1–5 % acetone in CH_2Cl_2) to give product **12** as a white foam (530 mg, 92 %). R_f = 0.50 (CH_2Cl_2/MeOH, 95:5, v/v); ^{1}H NMR (300 MHz, $CDCl_3$): δ = 8.56 (s, 1H; NH), 7.89–7.83 (m, 3H; H-6, Ph), 7.50–6.99 (m, 17H; triazole, Ph, pixyl), 6.24 (dd, J = 4.9, 8.5 Hz, 1H; H-1′), 4.16 (dd, J = 9.0, 12.9 Hz, 1H; H-6′), 3.79 (m, 1H; H-5′), 3.70 (dd, J = 3.6, 13.2 Hz, 1H; H-6′), 3.35 (br s, 1H; H-4′), 3.28 (d, J = 4.5 Hz, 1H; H-3′), 2.05 (s, 3H; CH_3(T)), 1.96 (m, 1H; H-2′), 1.78 (m, 1H; H-2′), 0.66 (s, 9H; C(CH_3)$_3$), −0.21 (s, 3H; $SiCH_3$), −0.32 ppm (s, 3H; $SiCH_3$); ^{13}C NMR (75 MHz, $CDCl_3$): δ = 163.7 (C-4), 152.2, 152.0 (pixyl), 150.3 (C-2), 147.8 (triazole), 146.3 (pixyl), 135.7 (C-6), 131.3, 130.9, 130.6, 130.5, 128.9, 128.3, 127.8, 127.7, 125.8, 124.0, 122.9, 122.3, 120.7, 117.6, 117.2 (pixyl, triazole), 111.2 (C-5), 86.6 (C-4′), 84.7 (C-1′), 78.8 (pixyl), 73.1 (C-3′), 72.0 (C-5′), 50.1 (C-6′), 40.9 (C-2′), 25.6 (C(CH_3)$_3$), 17.7 (C(CH_3)$_3$), 12.8 (CH_3(T)), −4.6, −4.8 ppm (CH_3Si); HRMS (ESI): m/z: calcd for $C_{44}H_{47}N_5O_6SiNa^+$ [M+Na]$^+$: 792.3188; found: 792.3201.

Synthesis of 5′-(*S*)-*C*-(4-phenyl-1,2,3-triazol-1-yl)methyl-5′-*O*-pixylthymidine (13): A solution of TBAF in THF (1.0 M; 1 mL, 1.00 mmol) was added to a stirred solution of compound **12** (500 mg, 0.65 mmol) in anhydrous THF (8 mL). The reaction mixture was stirred at room temperature for 16 h. CH_2Cl_2 (50 mL) was added and the mixture was washed with water (30 mL). The aqueous phase was extracted with CH_2Cl_2 (3× 40 mL) and the combined organic phase was dried (Na_2SO_4) and concentrated under reduced pressure. The residue was purified by chromatography (0–5 % MeOH in CH_2Cl_2) to give product **14** as a white foam (300 mg, 70 %). R_f = 0.24 (CH_2Cl_2/MeOH, 95:5, v/v); ^{1}H NMR (300 MHz, [D_6]DMSO): δ = 11.38 (s, 1H; NH), 8.11 (s, 1H; triazole), 7.78–7.74 (m, 2H; Ph), 7.55 (s, 1H; H-6), 7.45–6.94 (m, 16H; Ph, pixyl), 5.6 (t, J = 6.6 Hz, 1H; H-1′), 4.99 (d, J = 4.2 Hz, 1H; OH-3′), 4.26 (dd, = 9.1, 14.8 Hz, 1H; JH-6′), 3.84–3.78 (m, 2H; H-5′, H-6′), 3.53 (m, 1H; H-3′), 3.20 (t, J = 2.4 Hz, 1H; H-4′), 1.95–1.91 (m, 2H; H-2′), 1.85 ppm (s, 3H; CH_3); ^{13}C NMR (75 MHz, [D_6]DMSO): δ = 163.6 (C-4), 151.0, 150.9 (pixyl), 150.2 (C-2), 147.3 (triazole), 146.0 (pixyl), 135.4 (C-6), 130.9, 130.5, 130.3, 130.2, 128.9, 128.8, 127.8, 127.1, 125.1, 123.8, 123.7, 122.4, 122.0, 116.7, 116.3 (pixyl, Ph, triazole), 109.7 (C-5), 84.9 (C-4′), 83.5 (C-1′), 77.2 (pixyl), 71.8 (C-5′), 70.0 (C-3′), 49.7 (C-6′), 40.0 (C-2′), 12.3 ppm (CH_3); HRMS (ESI): m/z: calcd For $C_{38}H_{33}N_5O_6Na^+$ [M+Na]$^+$: 678.2323; found: 678.2327.

Synthesis of 3′-*O*-(*P*-2-cyanoethoxy-*N*,*N*-diisopropylaminophosphinyl)-5′-(*S*)-*C*-(4-phenyl-1,2,3-triazol-1-yl)methyl-5′-*O*-pixylthymidine (14): *N*,*N*-Diisopropylethylamine (350 μL, 2.00 mmol) and 2-cyanoethyl-*N*,*N*-diisopropylphosphoramidochloridite (300 μL, 1.35 mmol) were added to a stirred solution of **13** (300 mg, 0.45 mmol) in anhydrous CH_2Cl_2 (5 mL), and the mixture was stirred at room temperature for 1 h. CH_2Cl_2 (30 mL) was added and the mixture was washed with a 10 % aqueous solution of $NaHCO_3$. The aqueous phase was extracted with CH_2Cl_2 (3×30 mL) and the combined organic phase was dried (Na_2SO_4) and concentrated under reduced pressure. The residue was purified by column chromatography (0.25 % pyridine and 0–1 % acetone in CH_2Cl_2) to give product **15** as a white foam (210 mg, 54 %). R_f = 0.47 (CH_2Cl_2/acetone, 9:1, v/v); ^{31}P NMR (75 MHz, $CDCl_3$): δ = 151.57 ppm; HRMS (ESI): m/z: calcd for $C_{47}H_{50}N_7O_7PNa^+$ [M+Na]$^+$: 878.3401; found: 878.3403.

Synthesis of 1*N*-benzoyl-5-ethynyluracil: Trimethylsilyl acetylene (725 μL, 5 mmol) and Et_3N (3 mL) were added to a mixture of 5-iodouracil (1.0 g, 4.2 mmol), [Pd(PPh_3)$_4$] (240 mg, 0.21 mmol) and CuI (65 mg, 0.34 mmol) in deoxygenated EtOAc (10 mL) under an Ar atmosphere. The mixture was stirred at room temperature for 5 h and then cooled to 0 °C. Filtration afforded a white solid (1.8 g), which was dissolved in a mixture of pyridine and MeCN (10 mL, 1:1, v/v). Benzoyl chloride (690 μL, 6.0 mmol) was added and the mixture was stirred at room temperature for 18 h. MeOH (1 mL) was added, and the mixture was concentrated under reduced pressure. The residue was purified by column chromatography (20–50 % EtOAc in petrol ether) to give 1*N*-benzoyl-5-(trimethylsilyl)ethynyluracil (1.15 g, 88 %); R_f = 0.4 (CH_2Cl_2/MeOH, 95:5, v/v); ^{1}H NMR (300 MHz, [D_6]DMSO): δ = 12.07 (br s, 1H; NH), 8.07 (s, 1H; H-6), 8.00 (q, J = 7.80 Hz, 2H; Bz), 7.78 (m, 1H; Bz), 7.60 (t, J = 7.50 Hz, 2H; Bz), 0.18 ppm (s, 9H; Si(CH_3)$_3$); ^{13}C NMR (75 MHz, [D_6]DMSO): δ = 169.1 (C=O), 161.3 (C-4), 148.9 (C-2), 147.3 (Bz), 135.5 (C-6), 131.0, 130.4, 129.4 (Bz), 97.7 (C≡C), 97.0 (C-5), 92.0 (C≡C), 0.0 ppm (Si(CH_3)$_3$); HRMS (ESI): m/z: calcd for $C_{16}H_{16}N_2O_3SiNa^+$ [M+Na]$^+$: 335.0828; found: 335.0822. A solution of TBAF in THF (1.0 M; 2 mL, 2 mmol) was added to a stirred solution of 1*N*-benzoyl-5-(trimethylsilyl)ethynyluracil (500 mg, 1.60 mmol) in THF (8 mL), and the reaction mixture was stirred at room temperature for 4 h. MeOH (2 mL) was added and the mixture was concentrated under reduced pressure. The residue was adsorbed on silica gel and purified by column chromatography (1–3 % MeOH in CH_2Cl_2) to give the product 1*N*-benzoyl-5-ethynyluracil as a colourless solid (325 mg, 85 %). R_f = 0.26 (CH_2Cl_2/MeOH, 95:5, v/v); ^{1}H NMR (300 MHz, [D_6]DMSO): δ = 12.05 (s, 1H; NH), 8.08 (s, 1H; H-6), 8.01 (m, 2H; H-Ar), 7.79 (t, J = 7.50 Hz, 1H; H-Ar), 7.60 (t, J = 7.80 Hz, 2H; H-Ar), 4.16 ppm (s, 1H; C≡CH); ^{13}C NMR (75 MHz, [D_6]DMSO): δ = 169.1 (C=O), 161.5 (C-4), 149.0 (C-2), 147.3 (Bz), 135.6 (C-6), 130.9, 130.4, 129.4 (Bz), 96.4 (C-5), 84.2, 75.5 ppm (C≡C); HRMS (MALDI): m/z: calcd for $C_{13}H_8N_2O_3Na^+$ [M+Na]$^+$: 263.0433; found: 263.0427.

Synthesis of 3′-*O*-(*tert*-butyldimethylsilyl)-5′-(*S*)-*C*-(4-(1*N*-benzoyluracil-5-yl)-1,2,3-triazol-1-yl)methyl-5′-*O*-pixyl-thymidine (15): Sodium ascor-

bate (135 mg, 0.67 mmol) and $CuSO_4 \cdot 5H_2O$ (90 mg, 0.18 mmol) were added to a stirred solution of compound **11** (590 mg, 0.88 mmol) and 1*N*-benzoyl-5-ethynyluracil (280 mg, 1.17 mmol) in a mixture of *t*BuOH, water and pyridine (12 mL, 5:5:2, v/v). The reaction mixture was stirred at room temperature for 24 h. CH_2Cl_2 (50 mL) was added and the mixture was washed with a 10% aqueous solution of $NaHCO_3$. The aqueous phase was extracted with CH_2Cl_2 (3×30 mL), and the combined organic phase was dried (Na_2SO_4) and concentrated under reduced pressure. The residue was purified by column chromatography (1–3% MeOH in CH_2Cl_2) to give product **15** as a white foam (650 mg, 81%). $R_f = 0.32$ (CH_2Cl_2/MeOH, 95:5, v/v); ^{1}H NMR (300 MHz, $CDCl_3$): $\delta = 10.37$ (br s, 1H; NH), 8.88 (s, 1H; NH), 8.28 (s, 1H; triazole), 7.98–7.95 (m, 2H; Bz), 7.83 (s, 1H; H-6), 7.67–7.64 (m, 2H; H-6, Bz), 7.53–6.96 (m, 15H; pixyl, Bz), 6.12 (dd, $J = 4.8$, 9.4 Hz, 1H; H-1′), 4.12 (dd, $J = 8.7$, 13.6 Hz, 1H; H-6′), 3.73–3.70 (m, 1H; H-5′), 3.60 (dd, $J = 3.6$, 13.6 Hz, 1H; H-6′), 3.35 (s, 1H; H-4′), 3.18 (d, $J = 4.8$ Hz, 1H; H-3′), 2.04 (s, 3H; CH_3(T)), 1.95 (m, 1H; H-2′), 1.80 (m, 1H; H-2′), 0.67 (s, 9H; $C(CH_3)_3$), −0.21 (s, 3H; CH_3Si), −0.32 ppm (s, 3H; CH_3Si); ^{13}C NMR (75 MHz, $CDCl_3$): $\delta = 168.4$ (C=O), 164.1, 160.7 (C-4), 152.0 (pixyl), 150.4, 150.2 (C-2_b), 146.1, 138.6, 138.6, 136.9, 135.9, 135.4, 131.4, 131.0, 130.6, 130.6, 129.4, 128.1, 127.7, 124.1, 124.0, 123.4, 122.9, 122.2 (C-6, tetrazole, Bz, pixyl), 117.5, 117.1 (pixyl), 110.8, 105.9 (C-5), 86.8 (C-4′), 85.0 (C-1′), 78.8 (pixyl), 73.3 (C-3′), 71.8 (C-5′), 50.4 (C-6′), 40.9 (C-2′), 25.7 ($C(CH_3)_3$), 17.7 ($C(CH_3)_3$), 12.8 (CH_3(T)), −4.5, −4.7 ppm (CH_3Si); HRMS (ESI): *m/z*: calcd for $C_{49}H_{49}N_7O_9SiNa^+$ $[M+Na]^+$: 930.3253; found: 930.3238.

Synthesis of 5′(*S*)-*C*-(4-(1*N*-benzoyluracil-5-yl)-1,2,3-triazol-1-yl)methyl-5′-*O*-pixyl-thymidine (16): A 1.0 M solution of TBAF in THF (1.0 mL, 1.0 mmol) was added to a stirred solution of compound **15** (575 mg, 0.52 mmol) in anhydrous THF (10 mL). The reaction mixture was stirred at room temperature for 24 h under Ar. CH_2Cl_2 (40 mL) was added and the mixture was washed with a 10% aqueous solution of $NaHCO_3$ (20 mL). The aqueous phase was extracted with CH_2Cl_2 (3×40 mL) and the combined organic phase was dried (Na_2SO_4) and concentrated under reduced pressure. The residue was purified by column chromatography (2–5% MeOH in CH_2Cl_2) to give product **16** as a white foam (424 mg, 86%). $R_f = 0.27$ (CH_2Cl_2/MeOH, 95:5, v/v); ^{1}H NMR (300 MHz, [D_6]DMSO): $\delta = 11.91$ (br s, 1H; NH), 11.35 (s, 1H; NH), 8.20 (s, 1H; triazole), 8.03 (d, $J = 7.2$ Hz, 2H; Bz), 7.89 (s, 1H; H-6), 7.80 (m, 1H; Bz), 7.61 (t, $J = 7.8$ Hz, 2H; Bz), 7.50 (s, 1H; H-6), 7.42–6.92 (m, 13H; pixyl), 5.90 (t, $J = 7.5$ Hz, 1H; H-1′), 4.98 (d, $J = 4.2$ Hz, 1H; OH-3′), 4.27 (dd, $J = 9.3$, 15.0 Hz, 1H; H-6′), 3.77–3.70 (m, 2H; H-6′, H-5′), 3.41 (m, 1H; H-3′), 3.15 (m, 1H; H-4′), 1.90–1.84 ppm (m, 5H; H-2′, CH_3); ^{13}C NMR (75 MHz, [D_6]DMSO): $\delta = 169.6$ (C=O), 163.7, 160.7 (C-4), 151.0, 150.9 (C-2), 150.2, 149.1, 147.1, 138.4, 138.2, 135.5, 135.4, 131.2, 130.9, 130.4, 129.5, 128.8, 128.1, 127.8, 125.3, 123.7, 123.6, 122.6, 122.4, 122.0 (C-6, tetrazole, Bz, pixyl), 116.7, 116.2 (pixyl), 109.5, 103.8 (C-5), 85.0 (C-4′), 83.6 (C-1′), 77.2 (pixyl), 71.8 (C-5′), 70.1 (C-3′), 49.5 (C-6′), 40.0 (C-2′), 12.3 ppm (CH_3); HRMS (ESI): *m/z*: calcd for $C_{43}H_{35}N_7O_9Na^+$ $[M+Na]^+$: 816.2388; found: 816.2407.

Synthesis of 5′-(*S*)-*C*-(4-(1*N*-benzoyluracil-5-yl)-1,2,3-triazol-1-yl)methyl-3′-*O*-(*P*-2-cyanoethoxy-*N*,*N*-diisopropylaminophosphinyl)-5′-*O*-pixylthymidine (17): *N*,*N*-Diisopropylethylamine (130 μL, 0.75 mmol) and 2-cyanoethyl-*N*,*N*-diisopropylphosphoramidochloridite (125 μL, 0.56 mmol) were added to a stirred solution of compound **16** (100 mg, 0.13 mmol) in anhydrous CH_2Cl_2 (2 mL). The reaction mixture was stirred at room temperature for 2 h. Then CH_2Cl_2 (30 mL) was added and the mixture was washed with a 10% aqueous solution of $NaHCO_3$. The aqueous phase was extracted with CH_2Cl_2 (3×30 mL) and the combined organic phase was dried (Na_2SO_4) and concentrated under reduced pressure. The residue was purified by column chromatography (0–20% acetone in CH_2Cl_2) to give product **17** as a white foam (90 mg, 70%). $R_f = 0.51$, 0.53 (CH_2Cl_2/acetone, 3:1, v/v); ^{31}P NMR (75 MHz, $CDCl_3$): $\delta = 151.92$, 151.13 ppm; HRMS (ESI): *m/z*: calcd for $C_{52}H_{52}N_9O_{10}PNa^+$ $[M+Na]^+$: 1016.3467; found: 1016.3513.

Synthesis of 3′-*O*-(*tert*-butyldimethylsilyl)-5′-*O*-pixyl-5′-(*S*)-*C*-(4-trimethylsilyl-1,2,3-triazol-1-yl)methylthymidine (18): Sodium ascorbate (15 mg, 0.15 mmol) and $CuSO_4 \cdot 5H_2O$ (10 mg, 0.021 mmol) were added to a stirred solution of compound **11** (200 mg, 0.30 mmol) and trimethylsilyl acetylene (TMSA; 43 μL, 0.30 mmol) in a mixture of *t*BuOH, water and pyridine (2.5 mL, 5:5:2, v/v). The reaction mixture was stirred at room temperature for 16 h. Additional portions of TMSA (43 μL, 0.30 mmol), sodium ascorbate (15 mg, 0.15 mmol) and $CuSO_4 \cdot 5H_2O$ (10 mg, 0.021 mmol) were added, and the reaction mixture was stirred for a further 3 h. CH_2Cl_2 (30 mL) was added and the mixture was washed with a 10% aqueous solution of $NaHCO_3$. The aqueous phase was extracted with CH_2Cl_2 (3×30 mL), and the combined organic phase was dried (Na_2SO_4) and concentrated under reduced pressure. The residue was purified by column chromatography (1–3% MeOH in CH_2Cl_2) to give product **18** as a white foam (203 mg, 88%). $R_f = 0.38$ (CH_2Cl_2/MeOH, 97.5:2.5, v/v); ^{1}H NMR (300 MHz, $CDCl_3$): $\delta = 8.55$ (s, 1H; NH), 7.78 (d, $J = 1.2$ Hz, 1H; H-6), 7.48–7.26 (m, 10H; triazole, pixyl), 7.13–6.98 (m, 4H; pixyl), 6.12 (dd, $J = 5.1$, 9.6 Hz, 1H; H-1′), 4.08 (dd, $J = 9.9$, 14.1 Hz, 1H; H-6′), 3.78–3.73 (m, 2H; H-6′, H-5′), 3.18–3.15 (m, 2H; H-4′, H-3′), 2.05 (d, $J = 0.6$ Hz, 3H; CH_3(T)), 1.90 (m, 1H; H-2′), 1.83 (m, 1H; H-2′), 0.68 (s, 9H; $C(CH_3)_3$), 0.27 (s, 9H; $Si(CH_3)_3$), −0.22 (s, 3H; CH_3Si), −0.34 ppm (s, 3H; CH_3Si); ^{13}C NMR (75 MHz, $CDCl_3$): $\delta = 163.7$ (C-4), 152.2, 151.9 (pixyl), 150.4 (C-2), 146.3 (triazole), 135.8 (C-6), 131.2, 130.8, 130.5, 130.0, 128.1, 127.7, 124.0, 123.9, 122.9, 122.3, 117.6, 117.1 (pixyl, triazole), 111.3 (C-5), 86.4 (C-4′), 84.5 (C-1′), 78.8 (pixyl), 72.9 (C-3′), 72.0 (C-5′), 49.2 (C-6′), 40.8 (C-2′), 25.6 ($C(CH_3)_3$), 17.7 ($C(CH_3)_3$), 12.8 (CH_3(T)), 1.0 ($Si(CH_3)_3$), −4.6, −4.8 ppm (CH_3Si); HRMS (ESI): *m/z*: calcd for $C_{41}H_{51}N_5O_6Si_2Na^+$ $[M+Na]^+$: 788.3270; found: 788.3232.

Synthesis of 5′-*O*-pixyl-5′-(*S*)-*C*-(1,2,3-triazol-1-yl)methylthymidine (19): A 1.0 M solution of TBAF in THF (2 mL, 2.00 mmol) was added to a stirred solution of compound **18** (350 mg, 0.44 mmol) in anhydrous THF (4 mL). The reaction mixture was stirred at room temperature for 55 h. CH_2Cl_2 (25 mL) was added and the mixture was washed with a 10% aqueous solution of $NaHCO_3$ (15 mL). The aqueous phase was extracted with CH_2Cl_2 (3×30 mL) and the combined organic phase was dried (Na_2SO_4) and concentrated under reduced pressure. The residue was purified by column chromatography (2–3% MeOH in CH_2Cl_2) to give product **19** as a white foam (250 mg, 94%). $R_f = 0.18$ (CH_2Cl_2/MeOH, 95:5, v/v); ^{1}H NMR (300 MHz, $CDCl_3$): $\delta = 9.36$ (s, 1H; NH), 7.57–7.00 (m, 16H; H-6, triazole, pixyl), 6.10 (t, $J = 6.9$ Hz, 1H; H-1′), 4.08 (dd, $J = 8.4$, 14.4 Hz, 1H; H-6′), 3.83–3.77 (m, 2H; H-6′, H-5′), 3.53 (m, 1H; H-3′), 3.30 (t, $J = 3.6$ Hz, 1H; H-4′), 2.82 (d, $J = 3.9$ Hz, 1H; OH-5′), 2.12 (m, 1H; H-2′), 2.00 (s, 3H; CH_3), 1.96 ppm (m, 1H; H-2′); ^{13}C NMR (75 MHz, $CDCl_3$): $\delta = 163.7$ (C-4), 152.0 (pixyl), 150.2 (C-2), 146.4 (pixyl), 136.0 (C-6), 133.9, 131.2, 131.2, 130.7, 130.4, 128.1, 127.6, 124.8, 124.0, 123.7, 122.6, 117.4, 116.9 (pixyl, triazole), 111.3 (C-5), 84.7 (C-4′), 84.0 (C-1′), 78.2 (pixyl), 71.1 (C-5′), 70.1 (C-3′), 49.9 (C-6′), 40.0 (C-2′), 12.8 ppm (CH_3); HRMS (ESI): *m/z*: calcd for $C_{32}H_{29}N_5O_6Na^+$ $[M+Na]^+$: 602.2010; found: 602.2040.

Synthesis of 3′-*O*-(*P*-2-cyanoethoxy-*N*,*N*-diisopropylaminophosphinyl)-5′-*O*-pixyl-5′-(*S*)-*C*-(1,2,3-triazol-1-yl)methylthymidine (20): *N*,*N*-Diisopropylethylamine (130 μL, 0.75 mmol) and 2-cyanoethyl-*N*,*N*-diisopropylphosphoramidochloridite (125 μL, 0.56 mmol) were added to a stirred solution of compound **19** (100 mg, 0.17 mmol) in anhydrous CH_2Cl_2 (2 mL). The reaction mixture was stirred at room temperature for 2 h. CH_2Cl_2 (30 mL) was added and the mixture was washed with a 10% aqueous solution of $NaHCO_3$. The aqueous phase was extracted with CH_2Cl_2 (3×30 mL) and the combined organic phase was dried (Na_2SO_4) and concentrated under reduced pressure. The residue was purified by column chromatography (0–2% acetone in CH_2Cl_2) to give product **20** as a white foam (81 mg, 60%). $R_f = 0.49$, 0.45 (CH_2Cl_2/acetone, 3:1, v/v); ^{31}P NMR (75 MHz, $CDCl_3$): $\delta = 151.48$, 151.23 ppm; HRMS (ESI): *m/z*: calcd for $C_{41}H_{46}N_7O_7PNa^+$ $[M+Na]^+$: 802.3089; found: 802.3086.

Synthesis of 3′-*O*-(*tert*-butyldimethylsilyl)-5′-(*S*)-*C*-(1-pivaloyloxymethyl-1,2,3-triazol-4-yl)methylthymidine (22): NaN_3 (335 mg, 5.15 mmol), sodium ascorbate (55 mg, 0.28 mmol), CuI (100 mg, 0.52 mmol) and *N*,*N*′-dimethylethylenediamine (80 μL, 0.75 mmol) were added to a stirred solution of pivaloyloxymethyl chloride (750 μL, 5.15 mmol) in a mixture of EtOH and water (8 mL, 7:3, v/v), and the reaction mixture was stirred under MW at 100 °C for 1 h. Then compound **21** (520 mg, 1.31 mmol), NaN_3 (335 mg, 5.15 mmol), sodium ascorbate (55 mg, 0.28 mmol), CuI (100 mg, 0.52 mmol) and *N*,*N*′-dimethylethylenediamine (80 μL,

0.75 mmol) were added, and the reaction mixture was stirred under MW at 100 °C for 30 min. The mixture was concentrated under reduced pressure and the residue was purified by column chromatography (0–2% MeOH in CH_2Cl_2) to give product **22** as a yellow foam (702 mg, 97%). R_f = 0.43 (CH_2Cl_2/MeOH, 9:1, v/v); ^{1}H NMR (300 MHz, $CDCl_3$): δ = 8.76 (s, 1H; NH), 7.72 (d, J = 1.2 Hz, 1H; H-6), 7.68 (s, 1H; triazole), 6.26 (dd, J = 6.0, 7.6 Hz, 1H; H-1′), 6.22 (s, 2H; OCH_2N), 4.55 (m, 1H; H-3′), 4.12 (d, J = 9.0 Hz, 1H; H-5′), 4.04 (br s, 1H; OH-5′), 3.85 (m, 1H; H-4′), 3.05 (dd, J = 9.4, 15.4 Hz, 1H; H-6′), 2.88 (dd, J = 3.6, 15.3 Hz, 1H; H-6′), 2.36 (m, 1H; H-2′), 2.17 (m, 1H; H-2′), 1.91 (d, J = 0.9 Hz, 3H; CH_3(T)), 1.19 (s, 9H; C(CH_3)$_3$), 0.88 (s, 9H; C(CH_3)$_3$), 0.07 (s, 3H; SiCH_3), 0.06 ppm (s, 3H; SiCH_3); ^{13}C NMR (75 MHz, $CDCl_3$): δ = 177.9 (C=O), 163.9 (C-4), 150.5 (C-2), 145.7 (triazole), 137.3 (C-6), 123.4 (triazole), 111.0 (C-5), 89.6 (C-4′), 86.7 (C-1′), 73.3 (C-3′), 70.4 (C-5′), 69.8 (OCH_2N), 40.5 (C-2′), 38.9 (C(CH$_3$)$_3$), 30.2 (C-6′), 26.9 (C(CH_3)$_3$), 25.8 (C(CH_3)$_3$), 17.7 (SiC(CH$_3$)$_3$), 12.7 (CH_3(T)), −4.5, −4.6 ppm (SiCH_3); HRMS (ESI): m/z: calcd for $C_{25}H_{41}N_5O_7SiNa^+$ $[M+Na]^+$: 574.2668; found: 574.2655.

Synthesis of 3′-*O*-(*tert*-butyldimethylsilyl)-5′-(*S*)-*C*-(1-pivaloyloxymethyl-1,2,3-triazol-4-yl)methyl-5′-*O*-pixylthymidine (23): Pixyl chloride (350 mg, 1.2 mmol) was added to a stirred solution of compound **22** (400 mg, 0.73 mmol) in anhydrous pyridine (6 mL). The reaction mixture was stirred at room temperature for 24 h, and another portion of pixyl chloride (175 mg, 0.6 mmol) was added. The reaction mixture was stirred at room temperature for 34 h, and a further portion of pixyl chloride (175 mg, 0.6 mmol) was added. The reaction mixture was stirred for another 10 h and CH_2Cl_2 (40 mL) was then added. The mixture was washed with a saturated aqueous solution of $NaHCO_3$ (30 mL). The aqueous phase was extracted with CH_2Cl_2 (3×30 mL) and the combined organic phase was dried (Na_2SO_4) and concentrated under reduced pressure. The residue was purified by column chromatography (0–3% MeOH in CH_2Cl_2) to give product **23** as a white foam (540 mg, 92%). R_f = 0.34 (CH_2Cl_2/MeOH, 95:5, v/v); ^{1}H NMR (300 MHz, $CDCl_3$): δ = 8.45 (s, 1H; NH), 7.88 (s, 1H; H-6), 7.46–7.21 (m, 10H; pixyl, triazole), 7.09–6.94 (m, 4H; pixyl), 6.20 (dd, J = 5.1, 9.3 Hz, 1H; H-1′), 6.10 (d, J = 4.2 Hz, 2H; OCH_2N), 3.57–3.56 (m, 2H; H-4′, H-5′), 3.37 (d, J = 4.5 Hz, 1H; H-3′), 2.87 (dd, J = 10.9, 13.9 Hz, 1H; H-6′), 2.10 (dd, J = 3.3, 14.4 Hz, 1H; H-6′), 2.05–1.98 (m, 4H; H-2′, CH_3(T)), 1.84 (m, 1H; H-2′), 1.17 (s, 9H; C-(CH$_3$)$_3$), 0.70 (s, 9H; C(CH$_3$)$_3$), −0.20 (s, 3H; SiCH_3), −0.31 ppm (s, 3H; SiCH_3); ^{13}C NMR (75 MHz, $CDCl_3$): δ = 177.7 (C=O), 163.8 (C-4), 152.1, 152.0 (pixyl), 150.2 (C-2), 146.9 (triazole), 144.4 (pixyl), 136.2 (C-6), 131.7, 130.8, 130.3, 130.1, 127.9, 127.8, 123.8, 123.8, 123.2, 123.0 (pixyl, triazole), 117.1, 116.9 (pixyl), 110.7 (C-5), 88.1 (C-4′), 85.2 (C-1′), 78.0 (pixyl), 74.0 (C-3′), 73.7 (C-5′), 69.6 (OCH_2N), 41.3 (C-2′), 38.8 (*C*-(CH$_3$)$_3$), 28.5 (C-6′), 26.9 (C(CH_3)$_3$), 25.7 (C(CH_3)$_3$), 17.8 (SiC(CH$_3$)$_3$), 12.8 (CH_3(T)), −4.7, −4.8 ppm (SiCH_3); HRMS (ESI) MS: m/z: calcd for $C_{44}H_{53}N_5O_8SiNa^+$ $[M+Na]^+$: 830.3556; found: 830.3527.

Synthesis of 5′-(*S*)-*C*-(1-pivaloyloxymethyl-1,2,3-triazol-4-yl)methyl-5′-*O*-pixyl-thymidine (24): A 1.0 M solution of TBAF in THF (1.25 mL, 1.25 mmol) was added to a stirred solution of compound **23** (680 mg, 0.84 mmol) in anhydrous THF (10 mL). The reaction mixture was stirred at room temperature for 5 h. CH_2Cl_2 (40 mL) was added, and the mixture was washed with a 50% aqueous solution of $NaHCO_3$ (40 mL). The aqueous phase was extracted with CH_2Cl_2 (3×40 mL) and the combined organic phase was dried (Na_2SO_4) and concentrated under reduced pressure. The residue was purified by column chromatography (0–5% MeOH in CH_2Cl_2) to give product **24** as a white foam (383 mg, 57%). R_f = 0.36 (CH_2Cl_2/MeOH, 9:1, v/v); ^{1}H NMR (300 MHz, $CDCl_3$): δ = 8.68 (s, 1H; NH), 7.44–6.90 (m, 15H; H-6, pixyl, triazole), 6.14 (d, J = 2.7 Hz, 2H; OCH_2N), 6.06 (t, J = 6.6 Hz, 1H; H-1′), 3.81 (m, 1H; H-3′), 3.62–3.56 (m, 2H; H-4′, H-5′), 3.15 (d, J = 2.7 Hz, 1H; OH-3′), 2.61 (dd, J = 8.1, 14.1 Hz, 1H; H-6′), 2.36 (m, 1H; H-6′), 2.19 (m, 1H; H-2′), 2.06–1.98 (m, 4H; CH_3, H-2′), 1.19 ppm (s, 9H; C(CH_3)$_3$); ^{13}C NMR (75 MHz, $CDCl_3$): δ = 177.8 (C=O), 163.8 (C-4), 152.0, 151.8 (pixyl), 150.1 (C-2), 136.1 (C-6), 147.4, 144.2, 131.7, 130.1, 129.8, 127.7, 127.2, 124.0, 123.6, 123.5, 123.2, 117.0, 116.4 (pixyl, triazole), 110.9 (C-5), 86.4 (C-4′), 83.9 (C-1′), 77.2 (pixyl), 72.9 (C-5′), 70.5 (C-3′), 69.6 (OCH_2N), 40.4 (C-2′), 38.9 (*C*-(CH$_3$)$_3$), 27.8 (C-6′), 26.9 (C(CH_3)$_3$), 12.8 ppm (CH_3(T)); HRMS (ESI): m/z: calcd for $C_{38}H_{39}N_5O_8Na^+$ $[M+Na]^+$: 716.2691; found: 716.2696.

Synthesis of 3′-*O*-(*P*-2-cyanoethoxy-*N*,*N*-diisopropylaminophosphinyl)-5′-(*S*)-*C*-(1-pivaloyloxymethyl-1,2,3-triazol-4-yl)methyl-5′-*O*-pixylthymidine (25): *N*,*N*-Diisopropylethylamine (260 μL, 1.50 mmol) and 2-cyanoethyl-*N*,*N*-diisopropylphosphoramidochloridite (250 μL, 1.12 mmol) were added to a stirred solution of **24** (200 mg, 0.29 mmol) in anhydrous CH_2Cl_2 (4 mL). The reaction mixture was stirred at room temperature for 1 h. CH_2Cl_2 (40 mL) was added and the mixture was washed with a 50% aqueous solution of $NaHCO_3$. The aqueous phase was extracted with CH_2Cl_2 (3×50 mL) and the combined organic phase was dried (Na_2SO_4) and concentrated under reduced pressure. The residue was purified by column chromatography (0–15% acetone in CH_2Cl_2) to give product **25** as a white foam (181 mg, 70%). R_f = 0.40, 0.34 (CH_2Cl_2/acetone, 9:1, v/v); ^{31}P NMR (121.4 MHz, $CDCl_3$): δ = 151.42, 150.26 ppm; HRMS (ESI): m/z: calcd for $C_{47}H_{56}N_7O_9PNa^+$ $[M+Na]^+$: 916.3769; found: 916.3757.

Oligonucleotide synthesis, hybridisation experiments and CD spectroscopy: The oligodeoxynucleotides were synthesised by using an automated Expedite 8909 nucleic acid synthesis system by following the phosphoramidite approach. Synthesis of oligonucleotides **K1**–**P6** were performed on the 0.2 μmol scale by using 2-cyanoethyl phosphoramidites of standard 2′-deoxynucleosides in combination with the modified phosphoramidites **9**, **14**, **17**, **20** and **25** as well as the known amidite of **2**.[5] The synthesis followed the regular protocol employing standard CPG supports and 1*H*-tetrazole as the activator. The modified amidites were manually coupled by using amidite (0.05 M) and tetrazol (0.5 M) as activator in CH_3CN for 20 min. The coupling yields for the modified phosphoramidites in combination with the following unmodified amidite were in the range of 32–100%. The 5′-*O*-DMT-ON oligonucleotides were removed from the solid support by treatment with concentrated aqueous ammonia at 55 °C for 16–24 h, which also removed the protecting groups. The oligonucleotides were purified by reversed-phase HPLC on a Waters 600 system by using an X_{terra} prep MS C18; 10 μm; 7.8×150 mm column; buffer: triethylammonium acetate (0.05 M); 0–70% buffer, 38 min; 70–100% buffer, 7 min; 100% buffer, 10 min. All fractions containing 5′-*O*-DMT protected oligonucleotide (t_R 20–30 min) were collected and concentrated. The products were detritylated by treatment with an 80% aqueous solution of acetic acid for 20 min, and finally isolated by precipitation with ethanol at −18 °C, overnight. After dissolution in double distilled water, the concentrations were determined spectrometrically at 260 nm in the pH 7.0 buffer assuming the following extinction coefficients; **K** ε_{260} = 17.0 (twice that of dT), **L** ε_{260} = 8.75 (dT + 0.25 for toluene[26]), **M** and **N** ε_{260} = 8.5 (same as dT), **O** ε_{260} = 12.5 (dT + 4.0 for the 4-(uracil-5-yl-)1,2,3-triazole),[19] **P** ε_{260} = 18.2 (dT + 9.7 for 4-methyl-1-phenyl-1,2,3-triazole[27]).

The UV melting experiments were carried out on a UV spectrometer. Samples were dissolved in a medium salt buffer containing Na_2HPO_4 (2.5 mM), NaH_2PO_4 (5 mM), NaCl (100 mM), and EDTA (0.1 mM) and adjusted to pH 7.0 with 1.0 μM concentrations of the two complementary sequences. The increase in absorbance at 260 nm as a function of time was recorded while the temperature was increased linearly from 5 to 75 °C at a rate of 0.5 °C min^{-1} by means of a Peltier temperature programmer. The melting temperature was determined as the local maximum of the first derivatives of the absorbance versus temperature curve. The melting curves were found to be reversible. All determinations are averages of at least duplicates within ±0.5 °C.

CD spectra were obtained at 5 °C by using the same medium salt buffer as in the UV melting experiments with 3.0 μM concentrations of the two complementary strands.

Molecular modelling

Parameterisation of modified nucleotides: The initial structures of the modified nucleotides (**K**, **L** and **O**) were built with the xleap program from the AMBER 9 suite.[28,29] Their geometries were optimised by using the Gaussian 03 program[30] at the Hartree–Fock level with the 6-31G* basis set. The electrostatic potentials of the optimised structures were calculated to allow determination of the restrained electrostatic potential (RESP) charges.[31] The rest of the force field parameters for the modified nucleotides were obtained from the general AMBER force field (GAFF)[32] by using the antechamber program from the AMBER 9 suite. Missing force field parameters were deduced by using the parmchk pro-

gram from the AMBER 9 suite, and by analogy between GAFF and the *ff99* parameters.[33] One modification was applied to the parameters to reproduce the ab initio energy profile for rotation between the uracil and triazole moieties of modification **O** (Figure S3 and Table S5 in the Supporting Information). The atom types used for modification **O** are shown in Figure S3 in the Supporting Information. For modifications **K** and **L** all atom types were taken from the *ff99* parameters.

MD simulations: All MD simulations were carried out with the AMBER 9 program suite[31,32] by using the *ff99*[33], *ff99-bsc0*[34] and GAFF[32] parameters for nucleic acids and ions. The TIP3P water model was used.[35] All starting coordinates were generated by using idealised B-DNA geometries except in one case (entry 15, Table 1) for which both idealised A- and B-DNA geometries were used. The additional units for the modified nucleotides were placed with a geometry in which they pointed away from the duplex. Net-neutralising Na^+ ions were added and the whole system was solvated in a truncated octahedron box filled with TIP3P water molecules. The edges of the periodic box were at least 12 Å away from the boundaries of the solute molecules. The lengths of edges of the periodic boxes were initially between 63 and 70 Å. For the initial equilibration, harmonic positional restraints with a force constant of 500 kcal mol^{-1} Å^{-2} were applied to the solute molecules and the system was minimised for 1000 steps of steepest descent minimisation. Thereafter, the force constant of the harmonic potential restraints was lowered to 10 kcal mol^{-1} Å^{-2} and a further 2500 steps of steepest descent minimisation was carried out. For the MD simulation, the SHAKE algorithm was applied with a 2 fs time step. The nonbond cut-off was 9 Å and the particle mesh Ewald method with default parameters was used to calculate long-range electrostatic interactions. The temperature of the system was raised from 0 to 300 K over 10 ps at constant volume by using Berendsen coupling algorithm with 1 ps time constant and applying harmonic positional restraints with a force constant of 10 kcal mol^{-1} Å^{-2} to the solute molecules. Initially, the system was equilibrated for 50 ps at 300 K and 1 atm with time constants of 1 and 2 ps, and finally production MD was run for 30 ns.

Analysis of the MD trajectories: The hydrogen bonds between modified nucleotides and the remainder of the duplex were analysed based on the following definition: the distance between the hydrogen bond acceptor and the electronegative atom bonded to the hydrogen atom is less than 3.1 Å, and the angle of the three atoms, the hydrogen bond acceptor, the hydrogen atom and the electronegative atom is between 150° and 180°. The occupying percentage of each hydrogen bond during the assigned period was calculated based upon the number of snapshots in which the definitions of the hydrogen bond are satisfied and the total number of snapshots. Snapshots were collected every 2 ps in the MD simulation. The minor groove width was calculated as the shortest interstrand phosphorus–phosphorus distance minus the van der Waals radius of two phosphate groups (5.8 Å).

Acknowledgements

The project was supported by The Danish Research Agency's Programme for Young Researchers, Nucleic Acid Center and The Danish National Research Foundation, The Danish Natural Science Research Council, Danish Center for Scientific Computing and Møllerens Fond. Birthe Haack and Christian Schneider are thanked for technical assistance.

[1] a) C. J. Leumann, *Bioorg. Med. Chem.* **2002**, *10*, 841–854; b) J. Wengel, *Org. Biomol. Chem.* **2004**, *2*, 277–280; c) K. V. Gothelf, T. H. LaBean, *Org. Biomol. Chem.* **2005**, *3*, 4023–4037; d) M. Endo, H. Sugiyama, *ChemBioChem* **2009**, *10*, 2420–2443; e) J. Chiba, M. Inouye, *Chem. Biodiversity* **2010**, *7*, 259–281.

[2] a) S. H. Weisbrod, A. Marx, *Chem. Commun.* **2008**, 5676–5685; b) P. M. E. Gramlich, C. T. Wirges, A. Manetto, T. Carell, *Angew. Chem.* **2008**, *120*, 8478–8487; *Angew. Chem. Int. Ed.* **2008**, *47*, 8350–8358.

[3] a) T. Nguyen, A. Brewer, E. Stulz, *Angew. Chem.* **2009**, *121*, 2008–2011; *Angew. Chem. Int. Ed.* **2009**, *48*, 1974–1977; b) R. Varghese, H.-A. Wagenknecht, *Chem. Commun.* **2009**, 2615–2624; c) V. L. Malinovskii, D. Wenger, R. Häner, *Chem. Soc. Rev.* **2010**, *39*, 410–422.

[4] S. L. Pedersen, P. Nielsen, *Org. Biomol. Chem.* **2005**, *3*, 3570–3575.

[5] M. S. Christensen, C. M. Madsen, P. Nielsen, *Org. Biomol. Chem.* **2007**, *5*, 1586–1594.

[6] C. Andersen, P. K. Sharma, M. S. Christensen, S. I. Steffansen, C. M. Madsen, P. Nielsen, *Org. Biomol. Chem.* **2008**, *6*, 3983–3988.

[7] T. Wu, K. Nauwelaerts, A. Van Aershot, M. Froeyen, E. Lescrinier, P. Herdewijn, *J. Org. Chem.* **2006**, *71*, 5423–5431.

[8] T. Umemoto, J. Wengel, A. S. Madsen, *Org. Biomol. Chem.* **2009**, *7*, 1793–1797.

[9] T. Wu, M. Froeyen, G. Schepers, K. Mullens, J. Rozenski, R. Busson, A. Van Aershot, P. Herdewijn, *Org. Lett.* **2004**, *6*, 51–54.

[10] M. S. Christensen, A. Bond, P. Nielsen, *Org. Biomol. Chem.* **2008**, *6*, 81–91.

[11] a) V. V. Rostovtsev, L. G. Green, V. V. Fokin, K. B. Sharpless, *Angew. Chem.* **2002**, *114*, 2708–2711; *Angew. Chem. Int. Ed.* **2002**, *41*, 2596–2599; b) C. W. Tornøe, C. Christensen, M. Meldal, *J. Org. Chem.* **2002**, *67*, 3057–3064.

[12] G. Wang, P. Middleton, *Tetrahedron Lett.* **1996**, *37*, 2739–2742.

[13] a) G. B. Payne, *Tetrahedron* **1962**, *18*, 763–765; b) M. L. A. von Holleben, P. R. Livotto, C. M. Schuch, *J. Braz. Chem. Soc.* **2001**, *12*, 42–46; c) J. Ravn, N. Thorup, P. Nielsen, *J. Chem. Soc. Perkin Trans. 1* **2001**, 1855–1861.

[14] a) W. A. Herrmann, R. W. Fischer, D. W. Marz, *Angew. Chem.* **1991**, *103*, 1706–1709; *Angew. Chem. Int. Ed. Engl.* **1991**, *30*, 1638–1641; b) W. A. Herrmann, R. W. Fischer, M. U. Rauch, W. Scherer, *J. Mol. Cat.* **1994**, *86*, 243–266; c) J. Rudolph, K. L. Reddy, J. P. Chiang, K. B. Sharpless, *J. Am. Chem. Soc.* **1997**, *119*, 6189–6190; d) G. S. Owens, J. Aries, M. M. Abu-Omar, *Catal. Today* **2000**, *55*, 317–363.

[15] G. Majetich, R. Hicks, G. R. Sun, P. McGill, *J. Org. Chem.* **1998**, *63*, 2564–2573.

[16] E. Nakamura, S. Mori, *Angew. Chem.* **2000**, *112*, 3902–3924; *Angew. Chem. Int. Ed.* **2000**, *39*, 3750–3771.

[17] Z. Janeba, J. Balzarini, G. Andrei, R. Snoeck, E. De Clercq, M. J. Robins, *Can. J. Chem.* **2006**, *84*, 580–586.

[18] L. Lolk, J. Pøhlsgaard, A. S. Jepsen, L. H. Hansen, H. Nielsen, S. I. Steffansen, L. Sparving, A. B. Nielsen, B. Vester, P. Nielsen, *J. Med. Chem.* **2008**, *51*, 4957–4967.

[19] P. Kočalka, N. K. Andersen, F. Jensen, P. Nielsen, *ChemBioChem* **2007**, *8*, 2106–2116.

[20] A. Rodger, B. Nordén, *Circular Dichroism and Linear Dichroism*, Oxford University Press, New York, **1997**.

[21] A. K. Saha, T. J. Caulfield, C. Hobbs, D. A. Upson, C. Waychunas, A. M. Yawman, *J. Org. Chem.* **1995**, *60*, 788–789.

[22] G. Wang, P. J. Middleton, C. Lin, Z. Pietrzkowski, *Bioorg. Med. Chem. Lett.* **1999**, *9*, 885–890.

[23] J. Fensholdt, J. Wengel, *Acta Chem. Scand.* **1996**, *50*, 1157–1163.

[24] a) H. Trafelet, E. Stultz, C. Leumann, *Helv. Chim. Acta* **2001**, *84*, 87–105; b) H. Trafelet, S. P. Parel, C. Leumann, *Helv. Chim. Acta* **2003**, *86*, 3671–3687.

[25] a) Z. Johar, A. Zahn, C. J. Leumann, B. Jaun, *Chem. Eur. J.* **2008**, *14*, 1080–1086; b) A. Zahn, C. J. Leumann, *Chem. Eur. J.* **2008**, *14*, 1087–1094; c) M. Kaufmann, M. Gisler, C. J. Leumann, *Angew. Chem.* **2009**, *121*, 3868–3871; *Angew. Chem. Int. Ed.* **2009**, *48*, 3810–3813.

[26] H. Destaillats, M. J. Chales, *J. Chem. Eng. Data* **2002**, *47*, 1481–1487.

[27] D. K. Wedegaertner, R. K. Kattak, I. Harrison, S. K. Cristie, *J. Org. Chem.* **1991**, *56*, 4463–4467.

[28] D. A. Pearlman, D. A. Case, J. W. Caldwell, W. S. Ross, T. E. Cheatham, S. Debolt, D. Ferguson, G. Seibel, P. Kollman, *Comp. Phys. Comm.* **1995**, *91*, 1–41.

[29] D. A. Case, T. E. Cheatham III, T. A. Darden, H. Gohlker, R. Luo, K. M. Merz, Jr., V. A. Onufriev, C. Simmerling, B. Wang, R. Woods, *J. Comput. Chem.* **2005**, *26*, 1668–1688.

[30] Gaussian 03, Revision D.02, M. J. Frisch, G. W. Trucks, H. B. Schlegel, G. E. Scuseria, M. A. Robb, J. R. Cheeseman, J. A. Montgomery, Jr., T. Vreven, K. N. Kudin, J. C. Burant, J. M. Millam, S. S. Iyengar, J. Tomasi, V. Barone, B. Mennucci, M. Cossi, G. Scalmani, N. Rega, G. A. Petersson, H. Nakatsuji, M. Hada, M. Ehara, K. Toyota, R. Fukuda, J. Hasegawa, M. Ishida, T. Nakajima, Y. Honda, O. Kitao, H. Nakai, M. Klene, X. Li, J. E. Knox, H. P. Hratchian, J. B. Cross, V. Bakken, C. Adamo, J. Jaramillo, R. Gomperts, R. E. Stratmann, O. Yazyev, A. J. Austin, R. Cammi, C. Pomelli, J. W. Ochterski, P. Y. Ayala, K. Morokuma, G. A. Voth, P. Salvador, J. J. Dannenberg, V. G. Zakrzewski, S. Dapprich, A. D. Daniels, M. C. Strain, O. Farkas, D. K. Malick, A. D. Rabuck, K. Raghavachari, J. B. Foresman, J. V. Ortiz, Q. Cui, A. G. Baboul, S. Clifford, J. Cioslowski, B. B. Stefanov, G. Liu, A. Liashenko, P. Piskorz, I. Komaromi, R. L. Martin, D. J. Fox, T. Keith, M. A. Al-Laham, C. Y. Peng, A. Nanayakkara, M. Challacombe, P. M. W. Gill, B. Johnson, W. Chen, M. W. Wong, C. Gonzalez, J. A. Pople, Gaussian, **2004**, Inc., Wallingford CT.

[31] C. I. Bayly, P. Cieplak, W. Cornell, P. A. Kollman, *J. Phys. Chem.* **1993**, *97*, 10269–10280.

[32] J. Wang, R. M. Wolf, J. W. Caldwell, P. A. Kollman, D. A. Case, *J. Comput. Chem.* **2004**, *25*, 1157–1174.

[33] J. Wang, P. Cieplak, P. A. Kollman, *J. Comput. Chem.* **2000**, *21*, 1049–1074.

[34] A. Perez, I. Marchan, D. Svozil, J. Sponer, T. E. Cheatham III, C. A. Laughton, M. Orozco, *Biophys. J.* **2007**, *92*, 3817–3829.

[35] W. L. Jorgensen, J. Chandrasekhar, J. D. Madura, R. W. Impey, M. L. Klein, *J. Chem. Phys.* **1983**, *79*, 926–935.

Received: May 10, 2010
Published online: September 30, 2010

